NTNU

Norwegian University of
Science and Technology

AC Electrical Breakdown Strength of Solid Solid Interfaces

A study about the effect of elasticity, pressure and interface conditions

Dimitrios Panagiotopoulos

Wind Energy
Submission date: October 2015
Supervisor: Erling Ildstad, ELKRAFT

Norwegian University of Science and Technology
Department of Electric Power Engineering

AC Electrical Breakdown Strength of Solid Solid Interfaces

A study about the effect of elasticity, pressure and interface conditions

Master of Science Thesis

For obtaining the degree of Master of Science in Electrical Engineering at Delft University of Technology and in Technology-Wind Energy at Norwegian University of Science and Technology.

Dimitrios Panagiotopoulos

15.10.2015

European Wind Energy Master - EWEM

Summary

In several electrical insulation components, such as cable connectors, joints and penetrators, various solid insulating materials are usually brought in contact, forming interfaces. The dielectric strength of these solid|solid interfaces is critical for the strength of the overall system. Especially in cases that the applied field has a tangential to the interface component, the solid|solid interface is regarded as a point of major weakness. Furthermore, these components are usually used in subsea applications and therefore the presence of water at the interface should be considered.

The primary objective of this work is to examine how the elasticity of the solid material, the applied pressure and the interface condition is influencing the 50Hz/AC breakdown strength of the interface with a tangentially applied field. First, an prediction of the effect of varying elasticity modulus on the breakdown strength is attempted through theoretical modelling, adding to existing work. Following, the assumptions are verified by experimental testing in the High Voltage Laboratory of the Norwegian University of Science and Technology (NTNU). In order to facilitate the execution of the tests, a customised setup is built in the laboratory and identical test-samples are produced and prepared. Different pressure levels are applied for each material combination (XLPE|XLPE, SIR|SIR or XLPE|SIR) and for each interface condition (dry, wet or lubricated). The test data are treated using the Weibull distribution and are compared based on the minimum, mean and 63^{rd} percentile value. It is seen that, generally, the minimum or the mean value is adequate to qualitatively compare the strength of different interfaces.

Through the tests, it is also seen that the softer the materials that form the interface are, the lower is the elasticity modulus and thus the higher the breakdown strength. The influence of water and insulating oil at the interface is also explored through experimental testing in the lab. Therefore, the breakdown strength of wet and

lubricated (oily) interfaces is examined and compared. Through analysing and accordingly presenting the test results, it becomes evident the the wet interface behaves poorly while the lubricated facilitates higher breakdown strength values. Further, the behaviour of an interface comprised by two materials with different elasticity is investigated (hybrid interface). The hybrid interface appeared to be the least affected by water, despite the low applied pressure.

Acknowledgements

This study was carried out at the Department of Electric Power Engineering of the Norwegian University of Technology (NTNU) under the co-supervision of the Electrical Engineering, Mathematics and Computer Science faculty of the Technical University of Delft (TU Delft). Also, the facilities of SINTEF Energy Research are utilised since this work is related to an ongoing SINTEF project about Subsea Power Supply (SUBCONN).

First, I would like to express my sincere gratitude to my supervisor at NTNU, prof. Erling Ildstad, head of the Department of Electric Power Engineering, for his trust, guidance and feedback during the execution of this work.

In addition, I wish to thank associate professor Dr.ir.Peter H.F. Morshuis and Dr. Armando Rodrigo Mor for undertaking the co-supervision of this work on behalf of TU Delft.

My parents and my siblings played a very significant role in this process. They did so, once again, by supporting me and by being truly beside me despite the physical distance, as they did for all the years of my studies. Therefore, I am thankful to them.

I would also like to thank my friends and colleagues for always being around with a good advice, food and coffee.

I wish to thank my partner J.R.J. who despite the circumstances is always there, giving me perspective and support.

Finally, I would like to express my deepest gratitude to the PhD candidate Emre Kantar (Department of Electrical Power Engineering, NTNU) for his invaluable

aid, support, guidance and feedback both in a professional and in a personal level.

Copenhagen, Denmark
15.10.2015

Dimitrios Panagiotopoulos

Contents

List of Figures

List of Tables

Nomenclature

Latin Symbols

d	Diameter of interfacial voids	[m]
E	Elasticity modulus (Young's modulus)	[Pa]
E'	Composite elasticity modulus	[Pa]
n	Number of interfacial contact spots	[-]

Greek Symbols

α	Weibull scale parameter	$[Vorsec]$
β	Weibull shape parameter	$[-]$
γ	Weibull location parameter	$[Vorsec]$
ν	Poisson's ratio	$[-]$

Abbreviations

AC	alternate current
cdf	cumulative distribution function

EPDM	Ethylene propylene diene terpolymer
IEC	International Electrotechnical Commission
IEEE	Institute of Electrical and Electronics Engineers
IREQ	Hydro-Québec's research institute
MLE	Maximum likelihood estimation
NTNU	Norwegian University of Science and Technology
SIR	Silicone rubber
XLPE	Cross-linked polyethylene

Chapter 1

Introduction

In this chapter a brief introduction in the subsea connector technology is made and the vulnerability of solid|solid interfaces is introduced. The scope of the thesis is presented and organised in the form of questions that set the objectives of this work. Finally, the structure of this document is presented, explaining the content of each chapter, in order to facilitate the reading process.

1.1 Subsea connectors

Subsea cable connectors are very vital components of oil and gas extraction and of future ocean renewable energy systems. They allow quick, reliable and in situ connection of offshore components to main parts while they provide versatility and modularity of expensive equipment and cables. However, cable connectors are often responsible for many failures and often act as the the bottleneck when designing new systems. [1] [2] [3]

Usually a distinction between subsea cable connectors is made according to their type; wet-mate connectors, dry-mate connectors and penetrators. Dry-mate connectors are of proven reliability and high rating but they require the connection to be made on the surface on a suitable for this purpose vessel - which is often expensive and tedious. Wet-mate connectors can be plugged in underwater, after all the equipment is in position. Even though here are several wet mate connector technologies developed by different companies, as a rule a pressurised dielectric fluid is used to to push the water away of the interfaces. This coexistence of dielectric fluids (insulating oils) and water is one of the reasons wet mate connectors can be problematic, as it is mentioned further. Subsea penetrators are more similar to bushings as they provide the interface between a cable and the wall of a device. The fact that one side of the penetrator is part of a usually bigger and robust device, allows higher voltage levers and water depths. However, high rated penetrators are used for more permanent applications. [1] [2] [3] [4]

A $10kV$ wet mate cable connector, a 3-phase $11kV$ wet mate cable connector, and a $60kV$ subsea penetrator is shown in figure 1.1, in figure 1.2 and in figure 1.3 respectively.

Figure 1.1: *Siemens SpecTRON 10, single phase 10KV, 630A max, wet mate cable connector for subsea pumping and compressing systems [5].*

Oil and gas industry

In oil and gas industry cable connectors have been used for years to power components such as pumps, motors and switchgears as well as to feed step-out wells.

Figure 1.2: *MacArtney Underwater Technology 3-phase 11KV, 400A continuous, wet mate cable connector for wave energy, tidal energy and floating wind energy applications [6].*

Figure 1.3: *Siemens SpecTRON 60, 60KV subsea penetrator (up tp 2000 meter depth) [5].*

Moreover, recent and future needs on subsea processing and flow assurance systems, such as direct electrical heating (DEH) and pipe-in-pipe (PIP), mandate developing connectors which will be able to withstand higher voltage levels, higher power ratings, higher temperatures, deeper waters and longer tie-backs. Commercially available wet mate cable connectors are up to $36kV$ but tested in practise are only up to $12kV$. Wet mate connectors up to $150kV$ should be available within the next decade to facilitate the development of planned projects. [1] [3].

Renewable industry

Subsea connectors are gaining a position in renewable industry as well. Offshore windfarms and especially future floating projects can benefit both economically and in time by using subsea, wet mate connectors. Array cables can be fast and easily connected to floating or future seabed substations, without the need of special vessels. Moreover, tidal energy systems can also benefit from using subsea connectors in the sense that it is no longer necessary to pull the cables on the surface to connect them. This allows easy and effective fixation of the cables on the seabed enabling them to withstand strong ocean currents. In both cases, new, high rated and deepwater cable connectors must be developed. [2] [7]

Considering the need of exploiting even the most remote oil or gas reservoir to cover the future energy needs as well as the possible development of tidal and floating wind energy solutions, the need for high rated, reliable cable connectors becomes evident. In particular, high rated (in terms of voltage, current and power) wet

mate connectors need to be developed within the next decade. Reliable wet mate connectors which cover the requirements can actively contribute in reducing the cost of installation and maintenance of offshore and subsea systems due to the ease of use and modularity they provide (especially ROV-less solutions). However, the harsh deep water sea conditions pose a serious threat to the connectors since water ingress can cause direct breakdowns when penetrating in the insulating liquids between solid-solid insulating interfaces or gradual damage by causing water treeing to the core of solid insulating materials. Therefore, there is a large knowledge gap than needs to be bridged related to finding suitable materials for HV subsea applications, examining the influence of water in liquid dielectric fluids and analysing the parameters that affect the breakdown strength of weak points of the insulating system (such as solid-solid interfaces) [1] [3].

1.2 Solid interfaces as weak points of cable connectors

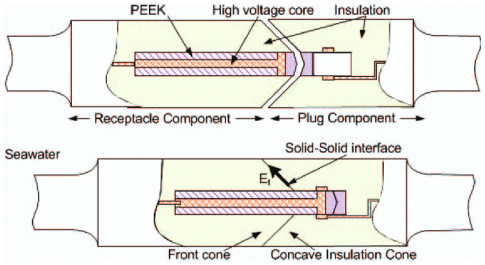

Figure 1.4: *Illustration of wet mate connector. The tangential field along the interface formed between the solid insulation parts is depicted in this simplified drawing [19].*

A simple illustration of a wet mate connector is depicted in figure 1.4. Except from the metallic contacts, solid insulating materials meet creating an interface. This interface must withstand the applied field which in most cases has a prevailing tangential component. Generally, these solid|solid interfaces act as weak areas of the equipment and are responsible for a significant percentage of failures [19].

It has been shown ([19]) that the breakdown strength and partial discharge inception voltage of the interface under field parallel to it is considerably lower than the breakdown strength of the bulk solid material. Partial discharges that are initiated on the interface lead to canonisation of the interface and eventually to breakdown.

The parameters that are considered critical for the breakdown strength and the level of the partial discharge inception voltage of the interface are the applied contact pressure, the material elasticity, the surface roughness, the possible lubrication of the interface, the water content in the lubricant or on the interface in the form of droplets and the existence of foreign particles. Moreover, the frequency of applied voltage add one more dimension to the problem. Even though current applications

nowadays use HVAC or HVDC technology, low voltage AC transmission has been proposed as well [23].

1.3 Solid interfaces in other insulating equipment

This work has been triggered by an ongoing project at SINTEF Energy Research on Power Insulation Material as part of the Subsea Power Supply Project [8]. Within the objectives of this project is the development of high voltage cable connectors in terms of voltage capability and reliability. Therefore, the starting point of this work is the existing cable connector technology. However, the study of solid|solid interfaces can be beneficial for a wider variety of insulating equipment such as cable joints and terminations.

1.4 Scope of the thesis

Research question

The majority of the currently used cable connectors operates primarily at 50Hz AC voltage. Therefore, even thought there is potential to other concepts (DC, low frequency AC), this work is restricted to the 50Hz AC. Also, solid|solid interfaces are particularly sensitive to the tangential component of the field. Therefore, the breakdown strength of the solid|solid interface on a tangentially applied field is investigated here.

The primary objective of this work is to examine the effect of elasticity, pressure and interface condition on the interfacial breakdown strength. Towards fulfilling this aim, a set of questions are raised and an attempt is made at their well-founded answer. These research questions are presented in this section.

What is the pressure dependence of the ac breakdown strength on dry interfaces formed by a softer material (silicon rubber)? The pressure dependence of the breakdown strength of XLPE|XLPE interfaces is already explored by previous work. It has been shown that higher applied pressure results in higher strength. Is this the case with - the softer - silicon rubber as well?

How does the elasticity modulus is expected to affect the breakdown strength of the interface?

How is the breakdown strength of the interface affected when combining XLPE and silicon rubber (hybrid interface)?

How does the presence of water in the interface affect the AC breakdown strength in each type of interface?

How does the presence of oil in the interface affect the AC breakdown strength in each type of interface?

Why does the presence of water or oil has this effect? What theoretical hypothesis supports it?

What would be an easy way to adequately compare breakdown data of different interfaces? Is it possible that the breakdown strengths of different interfaces are compared easily and without timely data manipulation?

Are the same breakdown mechanisms responsible for the breakdown regardless of the material? What conclusions can be reached by examining the interface surfaces after breakdown?

Thesis statement

The modulus of elasticity of the materials that form a solid|solid interface affects the 50Hz AC breakdown strength with tangentially to the interface applied field. More specifically, a more elastic material combination shows a higher breakdown strength. Theoretical estimation and experimental testing agree in this argument. Further, the presence of water in the interface is substantially decreasing the strength of the interface while a lubricated interface performs considerably better.

1.5 Structure

In chapter 2, a brief review on the relevant literature and existing work on the breakdown strength of solid|solid interfaces is presented. In addition to this, an introduction of the Weibull distribution and relevant terminology is made, which is considered necessary for the interpretation of the results.

Further, chapter 3 discusses and further develops an existing model (contact theory) that describes the breakdown of solid|solid interfaces. The existing model considers the applied mechanical pressure as a parameter. However, in this work the pressure is considered constant while the elasticity is the varying parameter. The contact theory is therefore manipulated so that the effect of the elasticity modulus on the breakdown strength becomes obvious and a theoretical background can be given to the experimental results.

The experiment setup and the test procedure that was followed in the lab is described in chapter 4. First, the custom-designed and constructed setup and all its components are presented in detail. The purpose of each part of the setup is then revealed in the step-by-step description of the experiment process.

In chapter 5 the preparation procedure of the XLPE and silicon rubber samples that were used in the experiments is presented. The procedure was different per material i.e. the XLPE was cut from an existing cable while the silicon rubber was produced in the lab. For both types of samples, the contact surfaces were prepared in the same way (grinding) so that they will have the same roughness and comparisons between interfaces become admissible.

The core of this work is chapter 6, where the experiment results are presented. The breakdown data is presented in Weibull plots and in terms of their minimum, mean and 63^{rd} percentile value. The results are divided primarily according to the interface condition (dry, wet, lubricated) and secondarily according to the type of interface (XLPE|XLPE, SIR|SIR, hybrid). Moreover, the test samples are examined under a microscope and the most reoccurring breakdown track patterns for every type of interface are documented.

Finally, in chapter 7 the results of this work are discussed and conclusions are made upon them.

Chapter 2

Literature review

In this chapter, a brief literature review on the breakdown strength of solid|solid interfaces is conducted. The literature review is divided in two sections, according to the institutes that the studies emerged from. Further, a thorough presentation is given of the Weibull distribution as means to represent breakdown data. This background is considered of importance because it facilitates the understanding of the Weibull plots, which are used widely for the presentation of results in this work.

2.1 Existing work

Great amount of research has been dedicated to the study of insulating materials, their breakdown strength and their applications in power engineering (cables, accessories, etc.). However, there are very few publications and little research on the characteristics of solid|solid interfaces as they appear in cable joints and connectors. These interfaces are considered the weak link in cabling systems and are responsible for the majority of failures [9] especially in cases where there is a significant tangential to the interface field component. Current designs for practical applications are based on experience and equipment testing. The majority of experimental results and research is restricted to studying complete designs of connectors or joints without isolating the interface. The breakdown along the interface of solids insulating is a complex phenomenon which is yet not fully investigated and explained [9]. Therefore, the specific parameters that influence the breakdown of solid|solid interfaces when the field is applied tangentially to the interface must be studied separately and especially in the case of polymers, which are the materials of choice in such applications.

2.1.1 The work at IREQ

A series of publications ([9] to [14]) on the subject of solid|solid interfaces have been made by Hydro-Québec's research institute, IREQ (Daniel Fournier et al.) in the 90's. The most relevant of them are presented briefly below.

Study 1 – Applied pressure and breakdown strength [9]

In this study [9] a modified Baur setup is used to measure the breakdown strength of a 4mm wide ethylene propylene diene terpolymer interface interface (EPDM|EPDM). Needle electrodes were used and weights were applied to achieve different levels of pressure. The set-up is illustrated in Figure 2.1.

Two cases were considered: (a) bare (dry) interface and (b) greased (lubricated) interface. In both cases it was shown that the breakdown strength is increasing with higher applied pressure (Figure 2.2).

Also, it was shown that the greased interface has considerably higher breakdown strength compared to the dry. Moreover, a different behaviour with increasing pressure was observed in the two cases. In the dry case, the breakdown strength shows a linear relationship with the pressure, while the greased saturates with increasing pressure (Figure 2.2).

It should be noted, however, that the above measurements were performed with pressures up to $0.8bar$, which represents only half the range of common operating pressures on EPDM|EPDM interfaces, i.e. $0.06 - 1.6bar$ [9].

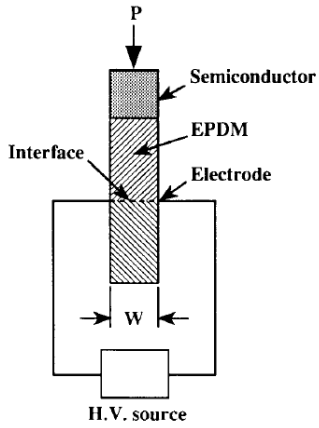

Figure 2.1: *Modified Baur set-up with needle electrodes for testing EPDM [9]. As seen the field is applied tangentially to the interface.*

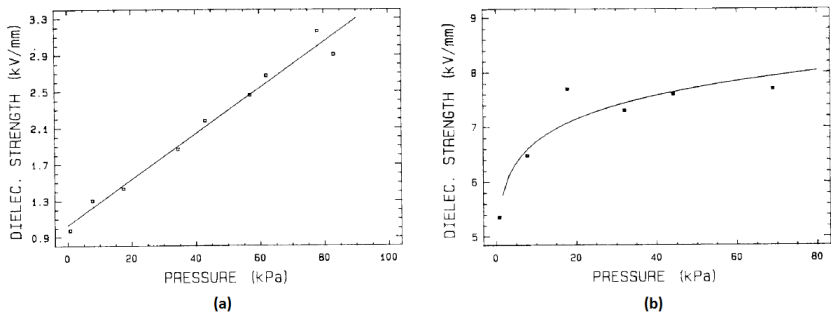

Figure 2.2: *Breakdown strength of dry (a) and greasy (b) EPDM interface [9].*

Study 2 – Surface roughness and breakdown strength [13]

In this work the test samples were slices which were cut from cable joints. The studied interfaces were EPDM|EPDM and EPDM|XLPE. Again, needle electrodes were used. In this case the interfaces were prepared in three different ways: no sanding, fine sanding (600grit) and normal (150grit) sanding. Also, both cases i.e. with and without grease in the interface, were examined.

Most of the conclusions regarding the roughness were about the effect it has on spreading uniformly and keeping the grease in place, which is not of relevant to the present study. However, a very useful conclusion can be deduced: in the study it was implied that EPDM|EPDM interface shows a better dielectric behaviour compared to EPDM|XLPE interfaces, where their strength depends on the grease used. Since EPDM is a softer than XLPE material, this result can support the assumption that the interface formed from softer materials (EPDM|EPDM) behaves

better than the interface formed from a material which is harder (EPDM|XLPE).

The above-mentioned studies consider EPDM interfaces under conditions similar to the operating (greased/non-greased, pressure levels). They provide the reader with a macroscopic, result-based set of conclusions. These direct and indirect conclusions raise a number of questions regarding the behaviour of solid|solid interfaces under different conditions and urge for a theoretical model to aid in their description. In the following section, a more systematic work on the subject is presented as it was performed at Norwegian University of Science and Technology.

2.1.2 The work at NTNU

A more systematic work, aiming directly towards the investigation of solid|solid interfaces, has been initiated at the Norwegian University of Science and Technology (NTNU), and SINTEF Energy. The most relevant points of this work are presented briefly in the following section as they constitute the ground and the starting point of this thesis.

Study 1 – Pressure and roughness effect on breakdown strength [18]

In this study the breakdown strength of XLPE|XLPE interfaces is investigated. This is performed both theoretically, by developing a describing model, and experimentally, by conducting breakdown tests. The pressure applied and the surface roughness are the varying parameters.

The theoretical approach is based on the argument that the micro-voids that are formed on the interface are responsible for partial discharge initiation and eventually lead breakdown. Application of mechanical contact theory leads to a model that can predict the breakdown strength of interfaces assembled in air. In short, by measuring the roughness, calculating the void size and number and knowing the applied pressure an estimation for the breakdown strength can be made. Two fundamental cases are considered: 1.the voids are ventilated (atmospheric pressure in the voids) and 2. the voids are not ventilated (increasing pressure in the voids). The model and its derivation is described in detail in section 3.2.

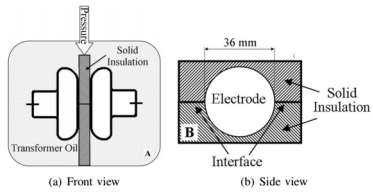

Figure 2.3: *Experimental set-up according to [18].*

For the experimental determination of the breakdown strength of XLPE|XLPE interfaces under varying applied pressure a simple set-up is utilised: two rectangular, 4mm thick, XLPE specimens are places between two Rogowski shaped electrodes and pressure is applied vertically perpendicular to the interface (Figure 2.3).

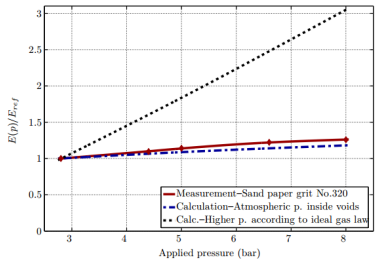

Figure 2.4: *Theoretical and measured results on breakdown strength of XLPE|XLPE interface with varying pressure as published in [18]. Increased applied pressure leads to increased breakdown strength.*

The study concluded that the breakdown strength of the XLPE|XLPE interface is increased with increasing applied pressure and by decreasing roughness [18] as seen in Figure 2.4. Also it showed that the breakdown values are consistent with the assumption of ventilated voids meaning that the pressure in the voids can be considered atmospheric. Finally, it was shown that assembling the interface in transformer oil instead of typical, dry, laboratory environment also increases the breakdown voltage. However, this result was not validated for different pressure levels.

This study is considered fundamental for the initiation of the present work.

Study 2 – Moisture and pressure effect on breakdown strength [19]

In continuation of the previous study, here, the influence of the applied pressure on the breakdown strength is also shown for interfaces assembled in water. The results are verified by using two different test setups: one as in Figure 2.3 and another using actual cable specimens.

An effort is put to extend the theoretical model in order to include water filled voids. In this direction, a distinction is made on the voltage drops across the voids and across the contact spots (Figure 2.5)

It is argued that the breakdown voltage of dry interfaces is the sum of the voltage drops across all the air-filled voids and across all the contact spots. On the contrary, the breakdown strength of the wet interface is the sum of the voltage drops across the contact spots only, since the voltage drop across the water filled cavities is considered zero.

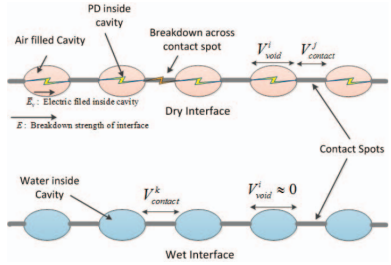

Figure 2.5: *Interfacial voltage drop along the interface as illustrated and analysed in [19].*

In this way, the total voltage drop across the air voids can be calculated by measuring the roughness characteristics of the surface, and afterwards compared to the difference between the measured breakdown strength of dry and wet interface.

This study concluded that water on the interface substantially decreases the breakdown strength. Also, it verified that increasing applied pressure causes increasing breakdown strength in both dry and wet conditions. Finally, it revealed the potential of the theoretical interface model, even though the need for improvements was acknowledged.

Study 3 – Sum of results [21]

In this study more details on the mechanical contact theory and surface characterisation are given, accompanied with some more experimental results using the set-up of Figure 2.3. The previous observations of the effect of roughness and pressure on the breakdown strength of dry interfaces are verified and supported by the theoretical model. This study effectively comprises and summarises results on the breakdown strength and partial discharge inception voltage of dry XLPE|XLPE interfaces.

The above studies try a more systematic approach including more variables (surface roughness, wet interface) and they also attempt a microscopic explanation of the phenomena through the theoretical modelling.

2.2 Weibull Distribution

The data produced by breakdown strength tests present a considerable scatter. Therefore, the manipulation of such results is performed with the use of statistical methods [31]. The most uncomplicated way is to use the normal distribution and represent each data set with the mean value. This is performed easily and the mean

value is also known as the 50% probability. However, especially in the case of designing high voltage equipment, values with much lower probability are of interest. Around the 50% probability the data usually fit well the normal distribution. Close to the tails of the distribution, the normal distribution seems to be ineffective, so it is preferable to use other distributions [32]. Different distributions have been used for this purpose (Weibull, Gumpel, lognormal, mixed) [30]. It is well studied and shown [24] that the best representation of breakdown data of solids is achieved by a Weibull probability distribution. Therefore, the Weibull distribution as well as its applicability, parameter estimation and use is presented in this section.

2.2.1 Definition

The Weibull distribution is a form of extreme value distribution, also described as "the weakest link" distribution. The general form of the Weibull cumulative distribution function (cdf) is the three-parameter Weibull distribution and is given by Equation 2.1.

$$P(u) = 1 - exp[-(\frac{u-\gamma}{\alpha})^{\beta}] \tag{2.1}$$

where,

u is the breakdown voltage[1] (or electric field) - the measured value or random variable

α is the (positive) scale parameter [same unit as the random variable]

β is the (positive) shape parameter [dimensionless]

γ the location parameter [same unit as the random variable]

The location parameter, γ, is attributed to the lowest voltage or time at which breakdown can occur. It is connected to a physical restriction that does not allow breakdown before that value. For example, the breakdown caused by electrical treeing may have a non zero location parameter which is justified as the minimum time needed for the tree to initiate and develop. Usually the location parameter is considered zero for simplicity, unless a clear reason to do otherwise exists [24] [31].

The Weibull cdf, $P(u)$, is often referred to as "unreliability" since $P(u)$ expresses the probability of breakdown at voltage equal or lower than u.

The special case of the three-parameter of the Weibull cdf where the location parameter, γ, is zero is called two-parameter Weibull distribution and is given by Equation 2.2.

$$P(u) = 1 - exp[-(\frac{u}{u_{63}})^{\beta}] \tag{2.2}$$

[1] Generally the random variable can be also the "time to breakdown", when dealing with duration tests. However, for this work only voltage tests are considered. Therefore, the random variable is referred to as "breakdown voltage".

where,

u_{63} is the (positive) scale parameter (same as α)

The voltage u_{63} is also referred to as the 63 percentile, the voltage where 63.2% of the tests result to breakdown. After the experimental breakdown data are gathered, it is convenient to fit them to a distribution so that they can be represented by the distribution's parameters. As it was mentioned earlier, the most commonly used ditribution is the Weibull.

2.2.2 Goodness of fit

When a set of data which follow the Weibull distribution is plotted on Weibull paper, then they will appear to be on a straight line. The Weibull paper is a linear plot of a transformation of the cdf's independent and dependent variables, after the natural logarithm of the reliability function $(1 - P(u))$ (Equation 2.2) is taken twice:

$$ln{-}ln[1 - P(u)] = -\beta ln(u63) + \beta ln(u) \tag{2.3}$$

After the transformation shown in Equation 2.4 and Equation 2.5, the Weibull distribution is a line with slope equal to the shape parameter, β.

$$x = ln(u) \tag{2.4}$$

and

$$y = ln{-}ln[1 - P(u)] \tag{2.5}$$

The values of unreliability, $P(u)$, are calculated according to the IEEE / IEC recommendations by Equation 2.6 [30].

$$P(i, n) \approx \frac{i - 0.44}{n + 0.25} \tag{2.6}$$

This type of representing the data on a Weibull paper is called Weibull plot. A straight line is fitted to the data using different techniques as it is seen below. Two examples of Weibull plots are illustrated in Figure 2.6 and Figure 2.7. In Figure 2.6, the Weibull data form sufficiently a straight line, whereas in Figure 2.7 the assumplion of the data forming a straight line is obviously erroneous[2].

[2]The curvature of the data points in Figure 2.7 towards the x-axis is an indication that the possibility of using a three-parameter Weibull distribution should be examined.

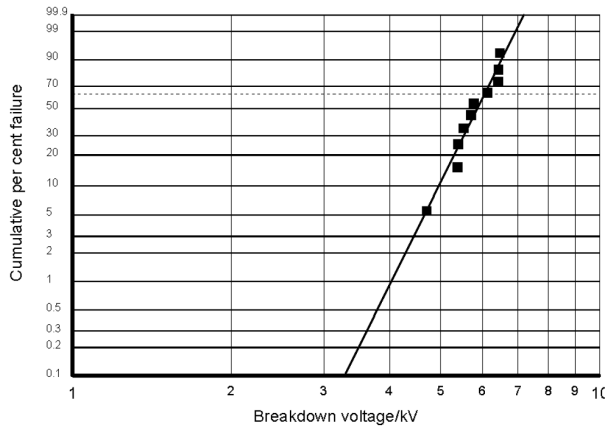

Figure 2.6: *Weibull plot of data that appear to adequately fit a two-parameter Weibull distribution (the data points form a fairly straight line) [30].*

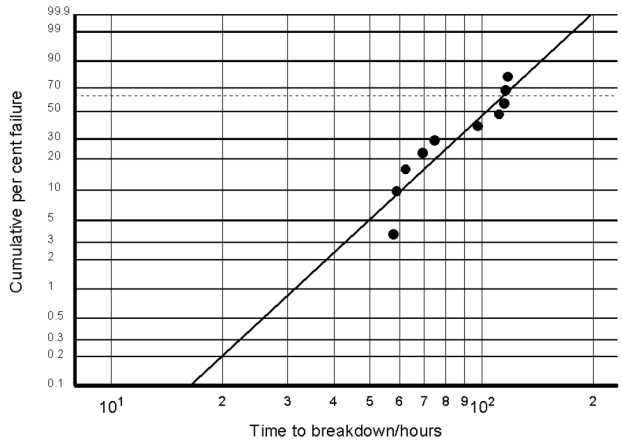

Figure 2.7: *Weibull plot of data that apparently do not fit a two-parameter Weibull distribution (the data points form a clearly curved line)[30].*

2.2.3 Parameter estimation

As it is mentioned earlier, it is desirable to refer to the breakdown data with the parameters of the distribution they fit. In this case the parameters are the shape factor β and the scale parameter u_{63}.

There are different methods used to estimate the parameters.

The simplest but least accurate way is the graphical estimation where a straight line is fitted "by eye" at the transformed data as plotted in the Weibull plot. The slope of the line is the shape parameter and the scale parameter is graphically

determined as the 63.5% value.

A computational and widely used method is the maximum likelihood estimate (MLE). MLE achives much more reliable parameter estimation than the graphical method [26]. However, according to IEC standards and IEEE suggestions [30] MLE appears to behave slightly biased.

IEC standards and IEEE [30] recommend the use of the simpler ([25]) least squares regression method. More specifically, for smaller data sets ($n < 20$), which is the case in this work, a variation is proposed which is called the White method. The White method allocates different weightings to each data point, calculates their weighted averages and through a simple formula estimates the parameters. The method is explained at [30].

2.2.4 Complete and censored data

The test data can be classified according to their integrity in three categories: complete, singly censored and progressively censored. When all specimens lead to breakdown the data is complete. Otherwise, when some of the tests do not lead to a breakdown, the data is referred to as censored. Singly censored data refer to data sets where the the tests where interrupted at a voltage value higher than the highest measured breakdown voltage. This kind of data occur usually when the upper limit of the voltage supply is reached and the test cannot be continued. In the case that one or more of the tests are interrupted for some other reason at any voltage, the data is referred to as progressively censored (suspended data). In any case, the censored data can and should be taken into consideration. IEEE/IEC standards [30] provide guidance on how each type of censored data can be handled. In order to achieve a representative parameter estimation, the censored data should not exceed the 30% of the total.

Chapter 3

The elasticity in the contact theory

The aim of this chapter is to theoretically examine the dependence of the interfacial breakdown strength on the elasticity of the material. This is achieved by developing an existing contact theory so that the elasticity becomes the varying parameter and then by showing the trend of the breakdown strength in a change of the elasticity. First, the size of the voids is linked through Paschen's curve to the breakdown of the interface. Subsequently the contact theory is presented and the relation of the elasticity to the size and number of interfacial cavities is developed. As a result, it is shown that if a more elastic material constitutes the interface, a higher breakdown strength is theoretically expected. Finally, a physical interpretation of the conclusion is attempted through some simplified illustrations.

3.1 Electrical breakdown along solid—solid interface

The interface formed by two flat solids pressed against each other is never perfect. The surfaces are not completely flat due to the asperities that are randomly distributed on them. Subsequently, there are cavities formed by the asperities which are in contact. The roughness of the surface is determined by shape and size of these asperities. The size and quantity of the formed voids depends on the applied pressure, the geometric characteristics of the asperities and the elasticity of the materials in contact [18] (more details given in section 3.2).

A simple model for the interface is introduced in [18] and describes the interface as a series connection of cavities and contact areas (Figure 2.5). Therefore, the voltage drop across the interface equals the sum of the voltage drops across the voids and the contact spots. Assuming air filled cavities, it is expected that the field will concentrate to the cavities (lower permitivity). The enhanced field initiates partial discharges in the cavities which lead to electrical breakdown [18]. It is argued ([18]) that the breakdown strength of the solid|solid interface is proportional to to the breakdown strength of the cavity.

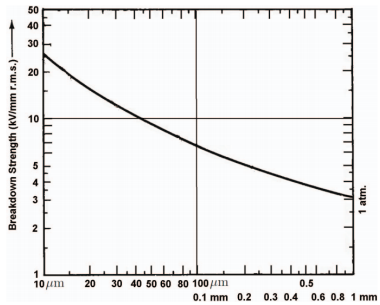

Figure 3.1: *Detail of Paschen's curve for air [19].*

The breakdown strength of an air filled cavity is governed by the breakdown strength of air which depends on the distance (here: void size) and the air pressure. This relation is described by Paschen's curve [33] (Figure 3.1 and Figure 3.2).

In previous work ([19]) it is shown that the interfacial voids are considered ventilated (atmospheric pressure). Therefore, in the attempt to analytically calculate or estimate the breakdown strength of the interface, it is sufficient to determine the expected size (and possibly shape) of the formed voids. Based on the principles of tribology, a contact theory has been proposed in [18] to determine the mean size of the voids on the interface. This approach is presented next, and following the influence of pressure and elasticity on the number and size of voids is determined.

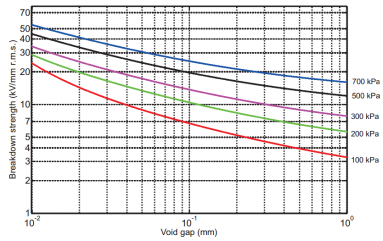

Figure 3.2: *Detail of Paschen's curve for air (plotted for different pressure levels) [21]*

3.2 Contact theory

3.2.1 Model formulation

According to the mechanical contact theory which is developed in [18], the voids are considered spherical so that a geometrical manipulation is analytically possible. In this way the diameter of the voids can be determined by calculating the number of voids and the total area that the voids occupy [18]. Regarding the number of voids, another assumption is made: the number of the voids is equal to the number of the contact spots. This assumption is necessary because according to the contact theory only the number of contact spots along the interface can be analytically estimated.

Equation 3.1 [18] yields the ratio between the real contact area A_{re} (microscopic) and the nominal contact area A (macroscopic). The nominal contact area is calculated by the size of the samples as the area of the side that is in contact, i.e. $4mm$ x $55mm$.

$$A_{re}/A \approx 2.4 \frac{p_a}{\left(E' \sqrt{\sigma/\beta}\right)} \tag{3.1}$$

Further, in Equation 3.1 the apparent applied pressure p_a, the composite elastic modulus E' (see subsection 3.3.1), the standard deviation of the the asperities' heights σ and the radius of the asperities' summit β are used.

Equation 3.2 [18] gives the number of contact spots and in extension the number of voids along the interface. Except from the already mentioned quantities, the surface density of the asperities [18] η is also used. The values of σ, β and η are determined my measuring the geometric characteristics of the interface surface (roughness). This measurement is performed using very sensitive profilometers (surface roughness characterisation equipment). However, the surface characteri-

sation falls out of the scope of this work.

$$n = 1.21\eta A \left(\frac{p_a}{(\eta\beta\sigma)\left(E'\sqrt{\sigma/\beta}\right)} \right)^{0.88} \tag{3.2}$$

The mean diameter of the spherical-assumed voids can be calculated with Equation 3.3 [18]. This equation involves the expected number of voids, n, and the total void area, $(A - A_{re})$.

$$d = 2\sqrt{\frac{A - A_{re}}{n\pi}} \tag{3.3}$$

Since the roughness of the surface is not a variable for this work (all samples are prepared with the same sandpaper), the quantities σ, β and η are considered constant regardless the material and they have, naturally, positive values. Considering the surface parameters constant is an important assumption that needs to be taken into account when comparing different materials.

3.2.2 Pressure dependence of breakdown strength

In order to examine the theoretical dependency of the breakdown strength to the applied pressure, the composite elastic modulus, E', is also taken as constant. This corresponds to interfaces of the same material, e.g. XLPE|XLPE. From Equation 3.2, it is seen that the higher the pressure the higher the number of the voids. Also, from Equation 3.1 and Equation 3.3, it is deduced that the higher the applied pressure the larger the real area of contact, A_{re}, and therefore the smaller the void size.

As deduced from Paschen's curve Figure 3.1, smaller voids imply a higher breakdown strength. Additionally, more voids also increase the breakdown strength. Therefore, it is seen qualitatively that increasing the pressure results in increasing the breakdown strength if the interface. This observation was also made in [18].

The aim of this chapter further, is to show a whether a similar deduction can be made for the elasticity of the material as a parameter, in order to predict and theoretically verify the experimental results of this work. The following section begins with a brief definition of some relevant terms related to the elasticity and continues with integrating the elasticity in the model equation and finally showing it influences the breakdown strength.

3.3 Elasticity in the contact theory

In this section, the effect of the varying elasticity on the breakdown strength of the interface is analysed through the contact theory. The composite elasticity becomes the varying parameter and its relation to the number and size of voids is shown. Subsequently and as it is mentioned previously, the size of the voids is the parameter that determines the breakdown strength. In this way the theoretical dependency of the interfacial breakdown strength on the material elasticity is revealed.

3.3.1 Composite elasticity

In Equation 3.1 and Equation 3.2, the composite elasticity E' is used for the calculation of the real contact area and for the number of asperities. In this section the composite elasticity is defined and calculated the the interfaces used in this work (XLPE|XLPE, SIR|SIR). First, the definition of the elasticity modulus and the Poisson's ratio is necessary.

Elasticity modulus

The elasticity modulus or Young's modulus, E, is defined as the ratio (slope) of the stress to the strain of the material in the elastic region of the stress - strain curve (Equation 3.4) [27]. The SI unit of the elasticity modulus is Pascal (for solids usually in the order of MPa / GPa).

$$E = \frac{\sigma}{\epsilon} \tag{3.4}$$

The elasticity modulus is a measure of the stiffness of a material [27]. The stiffer a material is, the higher the elasticity modulus. Alternatively, a more elastic material has a lower elasticity modulus, E.

Poisson's ratio

The negative ratio of the longitudinal elastic deformation due to a stress to the simultaneous lateral deformation is defined as the Poisson's ratio, ν, of the material [27]. The Poisson's ratio is dimensionless and positive[1]. For the majority of common materials the Poisson's ratio is in the range of $0 - 0.5$ [27].

[1] In reality, the Poisson's ratio can be negative for some (rare) material which are called auxetics.

Composite elasticity

In the contact theory that was unfolded previously, the composite elastic modulus, E', is used. The composite elastic modulus expresses the elastic modulus of the combination of two materials. As seen in [22], the composite elastic modulus is emerges from the elasticity moduli, E_1 and E_2, and Poisson's ratios, ν_1 and ν_2, of the materials in contact. The relation is described by Equation 3.5.

$$\frac{1}{E'} = \frac{(1-\nu_1)^2}{E_1} + \frac{(1-\nu_2)^2}{E_2} \tag{3.5}$$

In the special case that the materials in contact are the same, the moduli of elasticity E_1 and E_2 and the Poisson's ratios ν_1 and ν_2 are respectively equal and Equation 3.5 is simplified to Equation 3.8.

$$\frac{1}{E'} = 2\frac{(1-\nu)^2}{E} \tag{3.6}$$

For the scope of this work, the materials of interest are: XLPE and silicon rubber (SIR). The silicon rubber is chosen as a more elastic material to be compared to the stiffer XLPE. Quantitatively, the XLPE is assumed to behave mechanically similar to the low density polyethylene (LDPE), i.e. to have an elasticity modulus s $470MPa$ and a Poisson's ratio equal to 0.5 [19]. The elasticity modulus of the silicon rubber falls in the range $1 - 50MPa$ and the Poisson's ratio is $0.47 - 0.49$ [27].

In order to calculate the composite elasticity ,E', of each interface type, Equation 3.6 is used. For the XLPE|XLPE interface it is: $E = 470MPa$ and $\nu = 0.5$ and subsequently $E' = 940MPa$. For the SIR|SIR mean values are considered: $E = 25MPa$ and $\nu = 0.48$ and subsequently $E' = 46MPa$. Evidently, the SIR|SIR interface has a much lower composite elasticity modulus. This result will be of value in the next section, where the dependency of the breakdown strength on the elasticity will be explored.

3.3.2 Breakdown strength dependence on elasticity

By substituting Equation 3.1 and Equation 3.2 in Equation 3.3 an expression for the mean cavity diameter can be written. Considering that most of the quantities in these expressions are constant, a relatively simple expression is formed (Equation 3.7).

$$d = k_1\sqrt{E'^{0.88} - k_2 E'^{-0.12}} \tag{3.7}$$

where the constants k_1 and k_2 are given by Equation 3.8 and Equation 3.9.

$$k_1 = \frac{2\sqrt{\sigma/\beta}^{0.88}}{1.21\eta p_a^{0.88}} > 0 \tag{3.8}$$

$$k_2 = \frac{2.4p_a}{\sqrt{\sigma/\beta}} > 0 \tag{3.9}$$

To determine how the void size varies with the composite elasticity (and accordingly with the elasticity modulus), the equation Equation 3.7 is considered as a function of the composite elasticity that yields the void diameter. Following, the derivative of this function is taken. In Equation 3.10 it is shown that the derivative is positive, denoting that the function is ascending, meaning that for increasing composite elasticity, E', the mean diameter of the voids, d, is also increasing.

$$\frac{d}{dE'}d(E') = \frac{k_1(22E' + 3k_2)}{50E'^{1.12}\sqrt{E'^{0.88} - k_2E'^{=0.12}}} > 0 \tag{3.10}$$

As it was seen in subsection 3.3.1, the more elastic the material the lower the composite elasticity modulus. Utilising the conclusion of this section, it is estimated that the lower the composite elasticity, the smaller is the void size. As a result of the decreasing void size, higher breakdown strength is expected.

The previous paragraph is actually the essence of this chapter: it is shown that theoretically, based on the contact theory, the more elastic material is expected to have a higher interfacial breakdown strength.

Therefore, since the SIR|SIR has a lower composite elasticity than the XLPE|XLPE (as it is shown in the previous section), it it theoretically expected, according to the contact theory, that it will also have a higher breakdown strength.

3.3.3 Elasticity on void size and number - a physical interpretation

In this section the theoretical conclusion of the previous section is explained in a physical, more comprehensible way. According to the contact theory, a more elastic material results in a higher number of smaller voids. Smaller voids tend to have higher breakdown strength as described in Paschen's curve and therefore the interface is expected to withstand a higher field as well.

The contact surfaces that form the interface are not ideally flat and even, but they are characterised by asperities that depend on the surface preparation. It is assumed that for a certain surface preparation the asperities have a certain geometry (mean height and curvature of summits, average distance between summits etc) regardless the material.

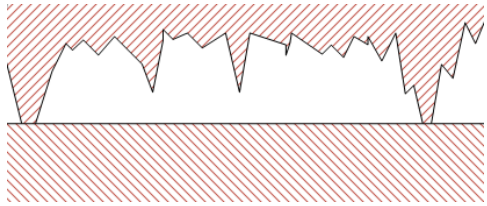

Figure 3.3: *Formation of interface cavities. The material in this case is hard (compared to Figure 3.4) and allows the formation of one large cavity. For simplicity the interface between a rough and an ideally flat surface is shown.*

Figure 3.3 and Figure 3.4 illustrate the same profile of a hard and soft material respectively being in contact with an ideally flat and stiff surface. The ideally flat surface is considered in order to simplify the illustration. As it is seen in Figure 3.3, the taller summits come in contact with the surface first and one large cavity is formed on this part of the interface. On the other hand, as seen in Figure 3.4, the material is softer and the tall summits are compressed so that more summits reach the flat surface. As a result, in the same section as before, there are now three, smaller cavities. Considering, now, the Paschen's curve (Figure 3.1), having more and smaller cavities means more and smaller air gaps and thus higher breakdown strength over a longer total distance. Therefore, the interface made of a softer material is expected to be able to withstand higher applied voltage.

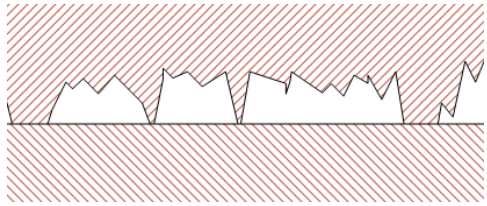

Figure 3.4: *Formation of interface cavities. The material in this case is soft (compared to Figure 3.3) and allows the formation of three small cavities. For simplicity the interface between a rough and an ideally flat surface is shown.*

The use of a more elastic material is expected to have a similar effect as applying more pressure has. Figure 3.3 and Figure 3.4 could as easily depict the same interface from the same material in the case that low and high mating pressure is applied respectively. Instead of considering a softer material responsible for the creation of more cavities, it is considered that the applied pressure forces the tall summits to compress. Therefore, the same qualitative explanation of this section holds for the higher strength of interfaces with higher applied pressure.

Chapter 4

Test Setup and Experiment Procedure

This chapter provides a detailed description of the test setup and the experiment procedure that was followed for the determination of the breakdown strength of solid|solid interfaces for tangentially applied 50Hz/AC field under various conditions. The setup that accommodates the test samples is designed in the lab and every aspect of it is presented along with the voltage supplying arrangement. Moreover, every step of the laboratory procedure during the tests is outlined and illustrated in a thorough flowchart.

4.1 Test Setup

In order to examine the breakdown strength of solid|solid interfaces under the influence of tangential to the interface field, a simple test setup is designed and constructed. Essentially, two rectangular prisms of XLPE or silicone rubber (SIR) are placed on top of each other - forming the interface - between two Rogowski shaped electrodes. , The rectangular prisms are 4mm thick, 55mm wide and 25mm tall (Table 4.1). The XLPE samples are cut from commercial XLPE cables, while the SIR are produced in the lab (chapter 5 is dedicated to the sample presentation). The prisms (samples) are pressed against each other vertically, so that the desired contact pressure is achieved. A simple illustration of the core of the test arrangement, as well as the dimensions of the basic components is seen in Figure 4.1.

Param	Value	Unit
height	25	$[mm]$
width	55	$[mm]$
thickness	4	$[mm]$

Table 4.1: *XLPE and SIR specimen dimensions*

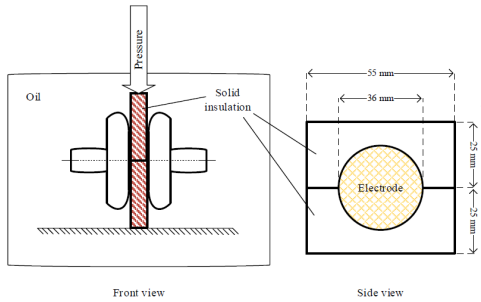

Figure 4.1: *Simple illustration of the test setup. The 4mm-thick solid insulator samples and the electrodes are depicted with their dimensions [29].*

The detailed arrangement of the test setup and photograph of the actual setup are shown in Figure 4.2 and Figure 4.3 . In the following, the numbers in parentheses refer to Figure 4.2. The 4mm-thick rectangular solid specimens (1) made of XLPE or SIR are placed on top of each other forming the interface (2). The two brass electrodes hold the specimens together with the aid of a helical compression spring (5) which pushes the moving electrode (4) against the fixed electrode (3). In this way the distance between the electrodes is restricted at the width of the specimens. The moving electrode is equipped with a wing nut (6) which acts as a handle to manually release the specimens between experiments.

The desired contact pressure at the interface is achieved by placing appropriate

weights (loads) (9) on the epoxy made moving weight-carrying plate (10). Different weights are used to achieve the desired pressure levels. Two steel guiding rods (11) are used to ensure the stability of the weight carrying plate. The plate applies pressure to the upper pressure dispersing block (12) which moves against the specimens. On the other side, the specimens are restricted by the fixed, lower pressure dispersing block (13). Both the pressure dispersing blocks are made of epoxy.

The produced AC high voltage is applied through the fixed electrode, while the moving electrode is grounded.

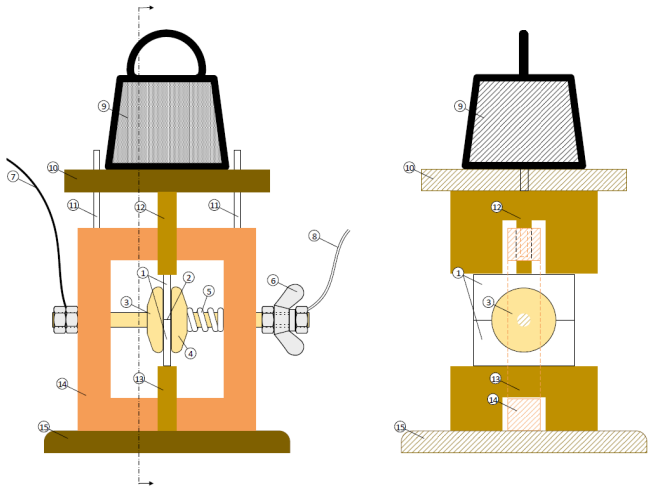

Figure 4.2: *Detailed llustration of the test setup. 1: rectangular solid specimens, 2: interface, 3:fixed electrode, 4: moving electrode, 5: spring, 6: wing nut, 7: high voltage wire, 8: earth wire, 9: weights, 10: moving weight-carrying plate, 11: guiding rods, 12: moving (upper) pressure dispersing block, 13: fixed (lower) pressure dispersing block, 14: supporting structure, 15: foundation*

The whole test setup is immersed in dielectric insulating fluid [34] to ensure that the breakdown will occur at the interface. The insulating oil considerably diminishes the probability of a breakdown along the surface and around the specimens or through the interface between the specimens and the pressure dispersing blocks. The dielectric insulating fluid used (MIDEL 7131) is a synthetic ester-based fluid with low environmental impact, increased fire safety, moisture tolerance and high dielectric strength [34]. The good dielectric properties of the oil are ensure by replacing the whole amount of it every 20 breakdowns.

As it is mentioned earlier, the field is applied across the interface through Rogowski shaped electrodes made of brass. This electrode profile is selected since it provides the best field uniformity compared to other profiles [35]. The Rogowski profile also minimises the field enhancement at the brim of the electrode [36]. The electric field and equipotential lines between the electrodes is depicted in Figure 4.4. The small

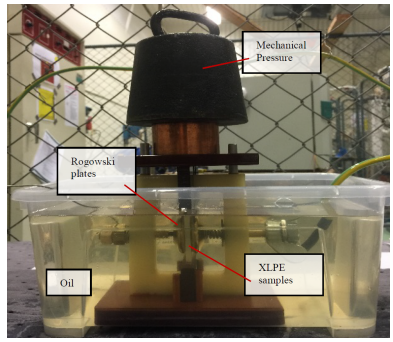

Figure 4.3: *The test setup as captured during the dry XLPE|XLPE testing. The samples are mated and mechanical pressure is applied while the setup is immersed in insulating oil. [29]*

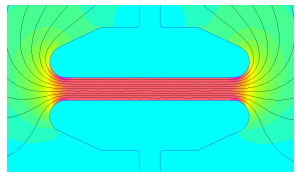

Figure 4.4: *Finite element calculation of the field and equipotential lines between the Rogowski shaped electrodes. The uniformity of the field between the electrodes is evident. The finite element calculation was performed with FEMM ([38])*

field enhancement is considered negligible, since most of the breakdowns occurred far from the edges.

The breakdown measurements are performed in the high voltage lab, in a cell surrounded by a metallic fence. In the cell the arrangement of Figure 4.5 is used. A PD-free transformer (1) with a ratio of 1:509 is used to supply the necessary high voltage. The ac voltage at the primary winding of the transformer is supplied from the grid (2) and is regulated by a variac. The variac is able to provide an increasing voltage with a certain rate that can be chosen in advance. Considering the expected voltage levels and the number of tests, the voltage rate is chosen to be $1kV/sec$. This rate falls within the range of short-time test, as it is defined in ASTM standards [17].

In order to restrict the breakdown current and protect the transformer, a water resistance (3) is used to supply the voltage to the test setup. The water resistance is basically a plastic tube filled with water and is confined at the two ends with conducting elements. Due to the fact that the water resistance is relatively heavy, a support insulator (4) is used to carry the weight. Finally, a thin wire (5) is used to supply the high voltage to the test setup.

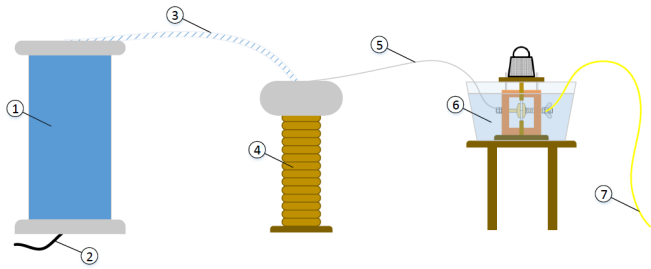

Figure 4.5: *Illustration of the overall test setup. 1:PD free transformer, 2: AC supply from variac, 3: water resistor, 4: support insulator, 5: supply of HV to setup, 6: setup in dielectric insulating liquid, 7: earth wire*

4.2 Experiment Procedure

The experiment procedure is described below step by step. Due to the large amount of tests, a well-described, systematic, thorough but in the same time simple procedure is of great value.

Before the experiments, all the specimens are prepared and stored in plastic bags (chapter 5).

Two new samples are taken and they assessed visually for imperfections and particles on the interface. Impaired samples are disregarded and in that case new samples are selected. If the forthcoming test is for a wet or lubricated interface, then the contact surface of the samples is instantaneously immersed in water or oil respectively. The samples are then being mated and placed between the electrodes. The whole setup is then moved in the empty basin. While keeping he moving electrode away from the samples so that no pressure is applied, the necessary weights are put on the weight-carrying plate. After the weights are placed and the samples are pressed against each other, the moving electrode is released and the basin is filled slowly with insulating oil.

At this point the setup is ready for the breakdown test so the earth stick is removed from the transformer and the door of the high voltage cell is closed. The voltage is gradually applied using the variac while a stopwatch is used to time the voltage increase (Figure 4.6) until the breakdown occurs. The breakdown voltage on the low voltage side of the transformer is measured with two regular voltmeters for redundancy. This value will later be referred to the high voltage side by using the transformer ratio. The time to breakdown measurement is used to monitor the rate of increase of the applied voltage. The measurements are documented in the lab log along with the date and the type of test (materials, condition of the interface).

The voltage is lowered to zero and the necessary safety measures are taken in order to enter the cell. After carefully removing the weights, the setup is taken out of the basin. To avoid waste of insulating oil it is important to allow enough time so that most of the oil drains in the basin. The specimens are removed from the

Figure 4.6: *The voltage regulator (variac) that supplies the test setup with increasing voltage of a fixed rate (1kV/sec).*

setup and they are assessed to verify that the breakdown occurred through the interface. If necessary notes are taken and the while the specimens are dried and marked for future reference. Finally, the electrodes are cleaned and dried of the oil using laboratory paper towels. The procedure continues by repeating the above steps until the tests are complete.

The procedure is summarised in the flowchart shown in Figure 4.7.

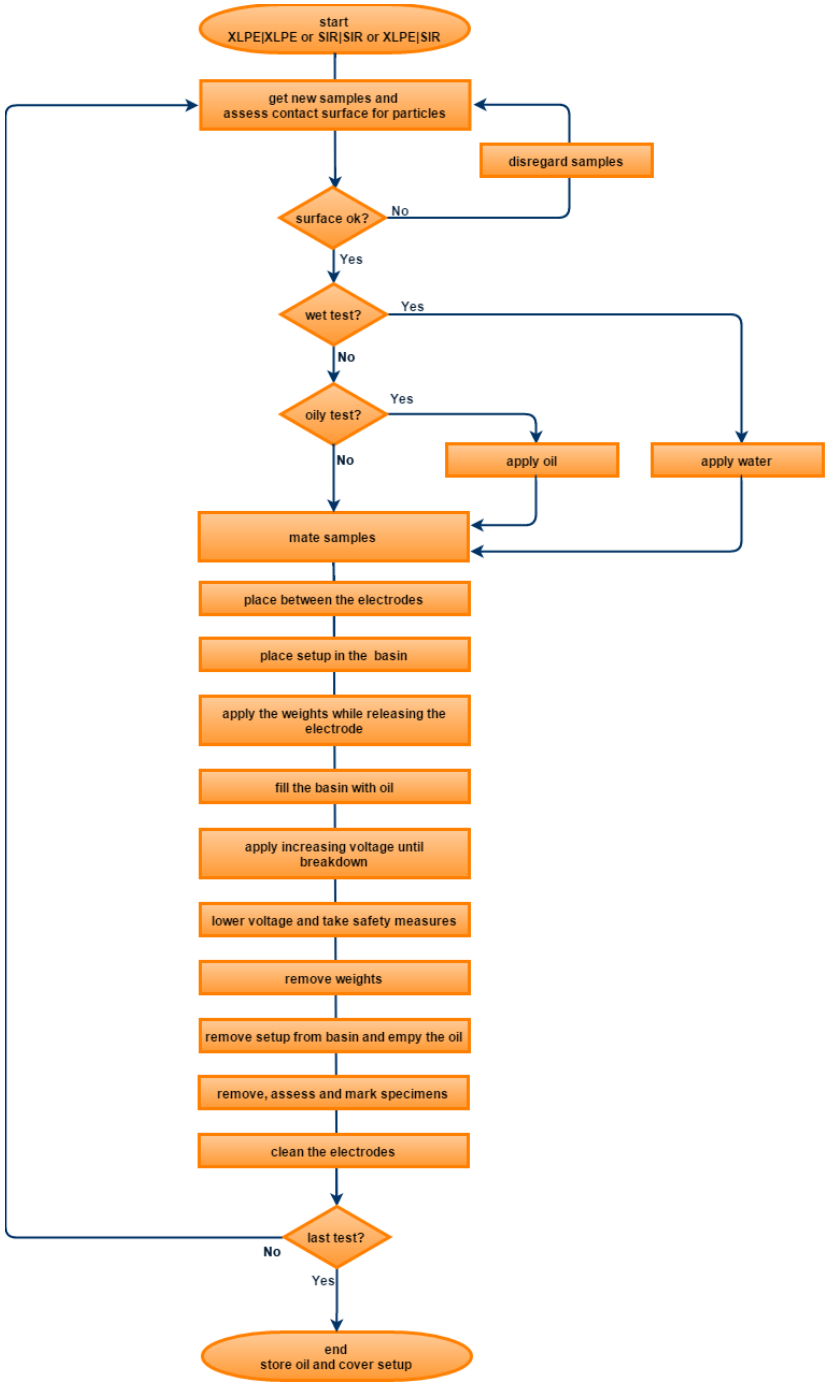

Figure 4.7: *Experiment procedure flowchart*

Chapter 5

Sample preparation

In this chapter the materials and the preparation procedure of the samples used in the experimental determination of the interfacial breakdown strength are presented. The setup used is introduced in chapter 4. In order to form the interfaces, rectangular prisms of XLPE and SIR are used which are 4mm thick, 55mm wide and 25mm tall (Table 4.1). In the case of XLPE, the samples are cut on the desirable size from a commercial cable, while the silicon rubber is produces in the lab. Moreover, the surfaces that form the interface need to be prepared in a certain way (grinding) to ensure that all interfaces are identical. The whole procedure is presented in this chapter and represents a substantial percentage of the total time dedicated to this work.

5.1 Formation of the samples

The procedure of creating the samples in the dimensions presented in Table 4.1 differs substantially from material to material. In the following sections, the preparation of the XLPE and SIR samples is presented analytically.

5.1.1 XLPE

The XLPE specimens are cut from a commercial high voltage cable. The nominal insulation thickness of the cable is $28mm$. The reason that an existing cable is used is that producing XLPE is challenging procedure which falls out of the scope of this work. Since only the behaviour of the interface is of interest, it is not critical to monitor and control the production of the XLPE. Therefore, the cable specimens are considered adequate. The insulation is separated from the conductor and $6cm$-long slices are cut along the conductor with a thickness of approximately $6mm$. For this a table saw is used in the workshop of NTNU lab.

Figure 5.1: *Preparation of XLPE samples. A table-knife is used for the fine cutting of the specimens before the surface preparation.*

The next step is to ensure that these coarse, $6cm$ long XLPE plates get a thickness of exactly $4mm$. For this purpose, a high accuracy carving machine is used to "scrap off" carefully the extra material and transform the coarse $6mm$-thick plates

into fine $4mm$-thick plates. However, these plates still do not have the necessary dimensions.

The $4mm$-thick XLPE is cut to the desired dimensions using a regular hand saw. The XLPE is hard enough to withstand the force of a saw and soft enough to be easily cut by hand. However, some experience with using saw is required, in order to achieve exact cuts. The specimens are prepared in bulk, by arranging them and pressing them together before cutting. It must be noted that the at this stage the height of the specimens is $27mm$ instead of $25mm$, to allow some extra length to be wasted during the fine cutting and grinding.

The fine cutting is performed by using a manual, horizontal table-knife/blade (Figure 5.1). Again, the specimens are placed in groups and thin slices are removed from the $4mmx55mm$ sides to ensure a perfectly flat surface, perpendicular to the sides.

At this point, the specimens have the necessary dimensions and are ready for the contact surface preparation (grinding).

Under physical examination, the XLPE samples are relatively hard, not brittle, opaque with a yellow-white colour, and have a characteristic smell, similar to the smell of plastic but more distinctive. Even thought XLPE is not toxic, a good ventilation while cutting it is suggested.

5.1.2 SIR

The silicon rubber used to make samples is prepared in the lab as a mixture of two viscous components. It is a silicon rubber under the commercial name ELASTOSIL®LR 3003/60 A/B by WACKER SILICONES [15]. The two components (A and B) are transparent liquids and they appear identical. They are both very viscous and therefore their treatment is challenging.

The mixture is made of the two components in equal quantities. As seen in Figure 5.2, a high accuracy electronic scale is used to measure the exact weight of each component. All equipment is cleaned with isopropanol and polyester/cellulose blend cleanroom wipers before the mixing procedure. Separate mixing sticks and a new pair of gloves is used for treating each material since contaminating each with the other should absolutely be avoided. The procedure takes place in a clean desk with forced ventilation.

In order to effectively mix the two components, a rotating mechanical stirrer under vacuum is used. The stirrer needs to have adequately big holes to avoid mechanical strain of the rotating equipment (Figure 5.3a). The mixing takes place under vacuum to minimise the creation of air bubbles in the mixture (Figure 5.3b). Overall, the mixing process takes about 2.5 hours and is performed in room temperature. Higher temperatures would aid the mixing by decreasing the viscosity but they should be avoided because they might accelerate the curing process.

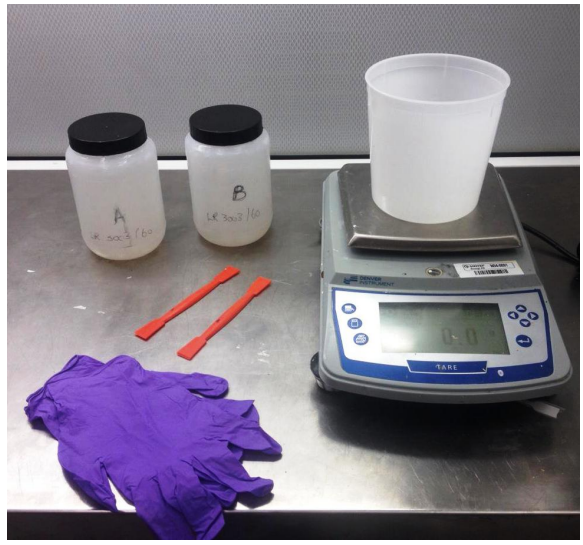

Figure 5.2: *Preparation of silicon rubber. An electronic scale is used to ensure equal quantities of the components A and B.*

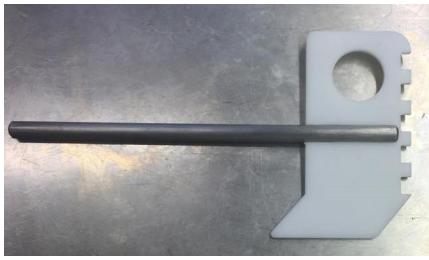

(a) For the mixing of the silicon rubber components a PTFE stirrer is used.

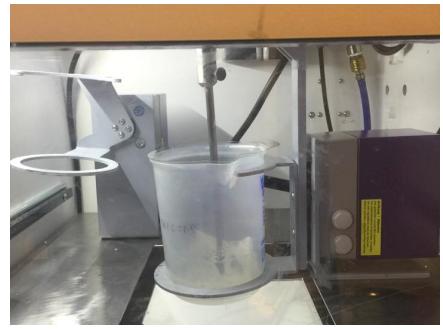

(b) The silicon rubber components, A and B, are mixed in a vacuum chamber.

Figure 5.3: *Mixing of silicon rubber.*

A steel mold (Figure 5.4a) in a heated press is used to shape the silicon rubber. The mold is essentially a square steel frame with thickness of $4mm$, and inner dimensions of $12cmx12cm$. It is placed on a heat resistant plastic foil and sufficient quantity of mixture is carefully placed in. Due to the high viscosity of the mixture, plastic foil is used to scoop it from the container to the mold. The procedure is performed with care so that the amount of air bubbles in the mixture is minimised. This requires some experience which is gained after the first few attempts. The mold is covered on top with the same plastic foil.

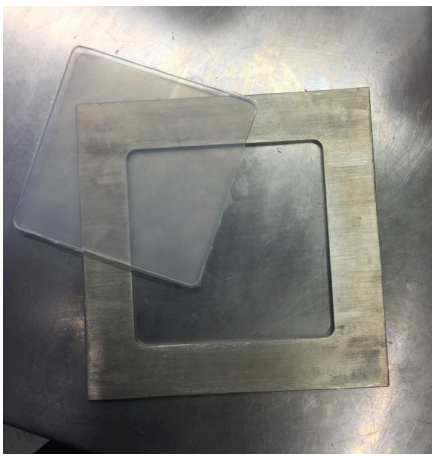

(a) Steel mold for silicon rubber molding.

(b) Mechanical press with temperature regulated plates for SIR molding.

Figure 5.4: *Molding of silicon rubber.*

The filled mold with the plastic covers is put in a press with temperature regulated plates (Figure 5.4b. Initially the plates are cold (room temperature) to avoid the initiation of the curing process before the full pressure is applied. First, low pressure is applied for two minutes so that the mixture spreads evenly in the mold. Following, there is high pressure applied in order to ensure the thickness of $4mm$. Simultaneously, the plates are heated, gradually up to 165 °C. The high pressure, heated cycle lasts 20 minutes and by the end of of the silicon rubber is cured. The plates are now cooled down by water circulation for 12 minutes so that the silicon rubber cools to room temperature. After the cooling is completed, the press releases the mold and the silicon rubber sample is removed.

The last step in the preparation of silicon rubber is the post curing. According to the data sheet [15], the post curing requires 4 hours in an ventilated oven of 200 °C. After the post curing, the 4mm-thick material (silicon rubber) is cut into rectangular prisms with a regular office paper trimmer. The samples have now the right dimensions and are ready to undergo the surface preparation (grinding).

5.2 Contact surface preparation

The preparation of the contact surface is presented in this section. Since the contact surface is not a varying parameter for this work, all interfaces need to be prepared in the same way. The preparation procedure needs to be strictly specified to ensure that all the specimens are identical. The contact surfaces are grinded and cleaned before the experiments as it is described below.

5.2.1 Grinding

The contact surfaces of the samples are prepared using a STRUERS Abramin [39] microprocessor controlled table top machine for automatic grinding, lapping and polishing. This is in essence a rotating grinding machine which uses SiC paper. As seen in Figure 5.5, the specimens are fixed on the steel rotating disk. A round, SiC, grinding paper sheet of grit No. 500 is also fixed on the rotating plane of the grinding machine. The rotating disk is then attached to the grinding machine and after adjusting the pressure and the time, the grinding takes place (Figure 5.6). During the process, water is being injected on the rotating plane to aid in removing the particles and avoid overheating and potentially melting of the materials.

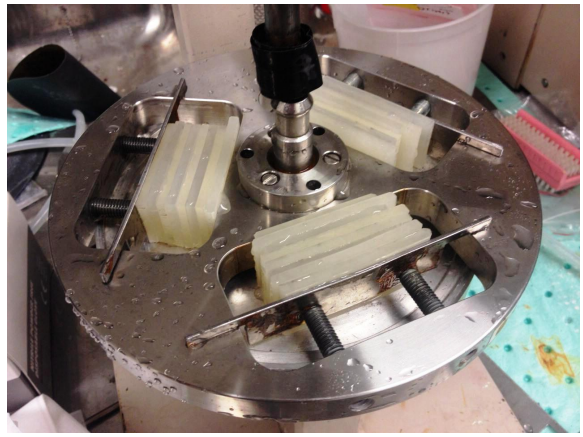

Figure 5.5: *Surface preparation of silicon rubber and XLPE samples. The samples are aligned and fixed on the rotating disc in order to be grinded.*

The XLPE and the silicon rubber behave differently due to the different elasticity. The XLPE is stiffer and therefore it stays easily fixed on the rotating disk. On the other hand, the silicon rubber is more flexible and the is being deformed while the grinding disk is rotating. After several attempts, it became obvious that the most effective way is to prepare the XLPE and SIR samples simultaneously by placing them alternately, as seen on Figure 5.5.

The samples are being grinded for approximately one minute with continuous flow of water so that the produced particles are removed. After this time they are assessed and if necessary they are grinded further.

5.2.2 Washing, drying and sealing

The prepared samples need to get cleaned and stored until the time they are used. First, the samples are rinsed in lukewarm water and they are left to dry on Polyester/cellulose blend cleanroom wipers in a clean, ventilated cupboard.

Figure 5.6: *The STRUERS Abramin rotating grinding machine while in use. The samples are being grinded while water is flowing.*

Subsequently, the dry samples are cleaned from any particles using compressed air. The clean samples are washed briefly in isopropanol using powder free-latex gloves to avoid recontamination. Finally, the samples are dried in a lab drier at approximately 50 °C for 5 minutes. In this way all the surface humidity is removed. The samples (specimens) are now ready and they are put in small, plastic, sealed bags until they are used. The number of specimens, the grit No., the material and the date of sealing is written on the bag using a permanent marker. This after treatment of the samples is a blend the procedures described in [16] and [19].

Chapter 6

Test data treatment and presentation of results

In this chapter the experiment results are presented and comments are made upon them. First, a description of the data manipulation is given in order to form a ground of understanding. Then the test results for the dry XLPE|XLPE, SIR|SIR and hybrid interface are presented and compared. The respective results for wet and lubricated interface follow in a similar manner. The results are analysed and observations are made which lead to conclusions that form the core of this work. Primarily, the results are compared in terms of their Weibull plots and subsequently also in terms of their mean and minimum value. This allows further conclusions to be made regarding the suitability of the mean and/or minimum value for comparing breakdown data sets. Finally, the used test samples are examined under an optical microscope and breakdown track patterns are recognised and presented.

6.1 Treatment of breakdown data

For each experiment, i.e. for each combination of materials, interface condition and pressure level, 7 tests are performed and in addition 2-3 in case that some of the measurements are disregarded after the breakdown.

In some cases, the breakdown does not happen though the interface but on the surface and through the insulating oil or through the material itself. These measurements are not disregarded; they are considered censored values and they are being treated accordingly. As a result, two types of data were emerged, i.e. complete data and singly censored data (see also section 2.2).

For the analysis of the breakdown data the Weibull distribution is used according to the IEC/IEEE recommendations ([30]). The Weibull plot is plotted for each set of data as described in section 2.2. The Weibull plot allows a visual comparison of the different experiments and the 63^{rd} percentile value facilitates a direct numerical comparison.

In previous works ([9] to [21]P), both the 63^{rd} percentile and the mean value have been used to represent and compare the AC breakdown values of solid|solid interfaces. The mean breakdown voltage is related with a Gaussian (normal) treatment of the data and is easy to calculate. On the other hand, the calculation of the 63^{rd} percentile value requires more effort but it does take into consideration the censored values.

Since a breakdown of the interface equals a breakdown of the equipment that it is part of, the minimum breakdown value is also of importance. The minimum value expresses a very low probability of breakdown, which in practical cases is of value. Also, when comparing many different cases, the simplicity of using the the minimum breakdown value to represent the whole data set might also be of value.

Therefore, in this work, all the three quantities, i.e. the minimum, the mean and the 63^{rd} percentile value, are used to compare the different cases.

6.2 Breakdown strength of dry interface

6.2.1 XLPE|XLPE interface

First, the breakdown behaviour of dry XLPE|XLPE interfaces is examined with varying pressure. More specifically 3 pressure levels were used: 5, 8.6 and 11.6 bar. Figure 6.1 depicts the Weibull plot of the breakdown strength of the dry samples and Figure 6.2 illustrates the minimum, mean and 63^{rd} percentile values for each pressure level.

As it is seen, the higher the applied pressure the slightly higher the breakdown strength in terms of all three indices (min, mean, 63%). More specifically, between 5 and 11.6 bar which corresponds to a 132% pressure increase, there is a 10%

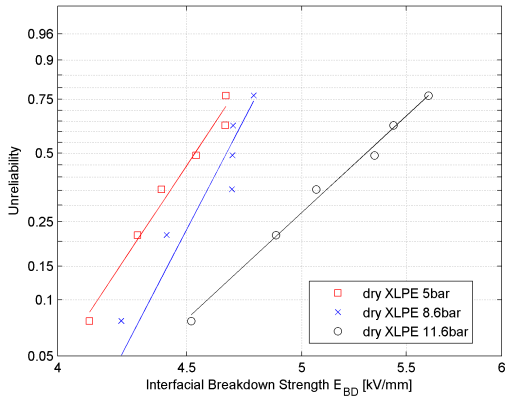

Figure 6.1: *Weibull plot of breakdown strength of dry XLPE|XLPE interface (5, 8.6 and 11.6 bar).*

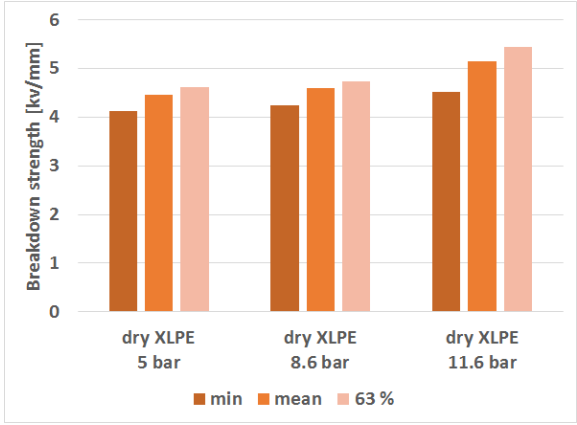

Figure 6.2: *Minimum, mean and 63^{rd} percentile breakdown strength of dry XLPE|XLPE interface (5, 8.6 and 11.6 bar).*

increase of the minimum breakdown value, 15% of the mean and 18% of the 63^{rd} percentile value. This increase is considered small, yet it is not questionable. This increasing tendency of the breakdown strength of dry XLPE|XLPE interface was also shown in [18] in terms of the 63^{rd} percentile. Even though the results of the two studies cannot be compared directly, there is logical agreement between them, which confirms the dependency of the interfacial pressure on the breakdown strength of dry-mated XLPE samples.

Except from the pressure levels shown in Figure 6.1 and Figure 6.2, the breakdown strength of the dry XLPE|XLPE interface was tested under a lower pressure, i.e. 2,7 bar. In this case, the breakdown strength values were unexpectedly higher

than in the case of 5 and 8.6 bar. This is justified as follows: with lower applied pressure, the interface was not tight enough and as a result some of the surrounding oil penetrated in the interface. This oil apparently increased slightly the breakdown voltage. The presence of some oil in the interface was verified after the tests. As a result this test is considered not useful for the examination of breakdown strength of dry interfaces and therefore is disregarded. As a solution to this problem in future works, it is suggested to use a more viscous insulating oil.

6.2.2 SIR|SIR interface

Since the purpose of this work is to examine the influence of the elasticity on the breakdown strength of solid|solid interfaces, the analogous tests are performed using instead of XLPE, the more elastic silicon rubber (SIR). The breakdown behaviour of dry SIR|SIR interfaces is examined with varying pressure. In this case 3 different pressure levels were used: 1.6, 1.9, 2.7 bar. The pressure levels are considerably lower than in the case of XLPE due to the more elastic nature of SIR. It was observed that applied pressure higher than about 2.7 bar is impractical because it caused considerable deformation of the rubber.

In Figure 6.3 the Weibull plot of the breakdown strength of the dry SIR samples is presented. Also, Figure 6.4 illustrates the minimum, mean and 63^{rd} percentile values for each pressure level, in the same way as for XLPE.

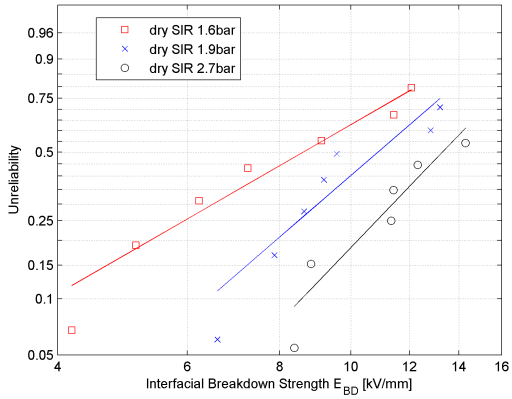

Figure 6.3: *Weibull plot of breakdown strength of dry SIR|SIR interface (1.6. 1.9 and 2.7 bar).*

It is observed again that the higher the applied pressure the higher the breakdown strength in terms of all three indices (min, mean and 63%).

More specifically, between 1.6 and 2.7 bar which corresponds to a 70% pressure increase, there is a 100% increase of the minimum breakdown value, 40% of the mean and 44% of the 63^{rd} percentile value. This is a noticeable increase which

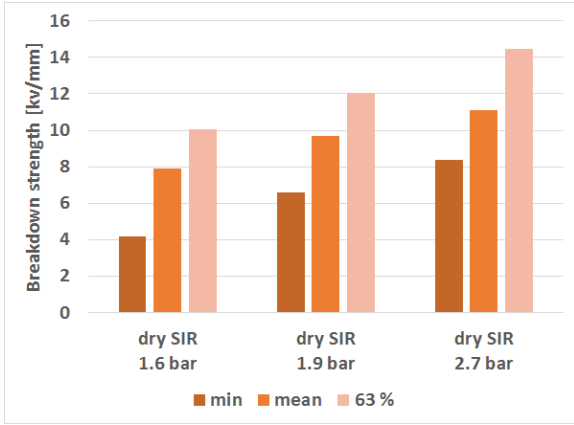

Figure 6.4: *Minimum, mean and 63^{rd} percentile breakdown strength of dry SIR|SIR interface (1.6. 1.9 and 2.7 bar).*

clearly verifies that for SIR|SIR interfaces the breakdown strength increases with increasing the applied pressure.

6.2.3 Comparison of dry XLPE|XLPE and SIR|SIR interface

In Figure 6.5 the Weibull plots of the breakdown strength of dry XLPE|XLPE and SIR|SIR interfaces are put under comparison. The same data sets are presented in terms of the three indices (min, mean and 63^{rd} percentile) in Figure 6.6.

It is evident that the dry SIR|SIR interface performs better than the dry XLPE|XLPE, even though the applied pressure is considerably lower.

More specifically, the 2.7 bar SIR|SIR dry interface shows a clearly superior behaviour compared to the XLPE|XLPE interfaces, despite the higher pressure applied to them. All indices (min, mean and 63^{rd} percentile) are respectively substantially increased indicating the higher breakdown strength. In the case of dry SIR|SIR interface with lower pressure, i.e. 1.6 bar, again higher breakdown strength is generally observed, except in terms of the minimum value. The minimum value is comparable and lower from the breakdown values of XLPE|XLPE interface. This indicates that the SIR|SIR dry interface under lower pressure is not necessarily able to withstand higher voltages than the XLPE|XLPE, even though it tends to behave better.

Another observation on Figure 6.5 is that the increasing pressure has relatively higher impact on the breakdown strength of dry SIR interfaces rather than of XLPE. According to the experimental results, for XLPE|XLPE interface a pressure increase from 5 to 11 bar, which corresponds to an increase of 120%, yields a increase of only 16% of the mean breakdown strength. However, a relatively smaller increase of the pressure applied on the SIR|SIR interface, from 1.6 to 2.7 bar, i.e.

67%, yields a much higher increase of the mean breakdown strength which is about 40%.

Finally, one significant observation on Figure 6.5 is the higher dispersion of breakdown values of SIR|SIR interface compared to XLPE|XLPE interface. In the XLPE case, relatively low dispersion of measurements is observed, with relative standard deviation 5% and 8% respectively, which is increasing with pressure. On the other hand, for SIR, high dispersion is noted, with relative standard deviation of 39% and 20%, which is decreasing with increasing pressure. This leads to the conclusion that for dry SIR|SIR interface the breakdown strength varies considerably and that for XLPE|XLPE it is much more "predictable", in the sense that the lowest and highest values are relatively close to each other.

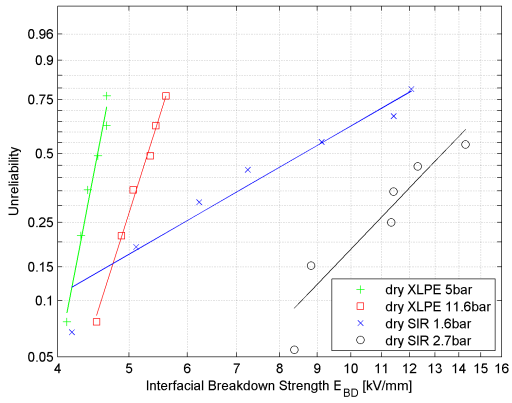

Figure 6.5: *Weibull plot of breakdown strength of dry XLPE|XLPE and SIR|SIR interface. Two different pressure levels for each material are shown.*

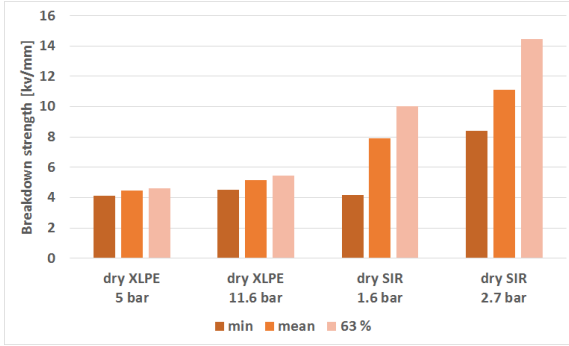

Figure 6.6: *Minimum, mean and 63^{rd} percentile breakdown strength of dry XLPE|XLPE and SIR|SIR interface (two pressure levels for each interface).*

All above considered, dry SIR|SIR interface shows higher breakdown strength despite the much lower applied pressure compared to dry XLPE|XLPE interface.

However, SIR|SIR interface breakdown values show a high dispersion which will increase the uncertainty when designing equipment.

6.2.4 Hybrid dry interface

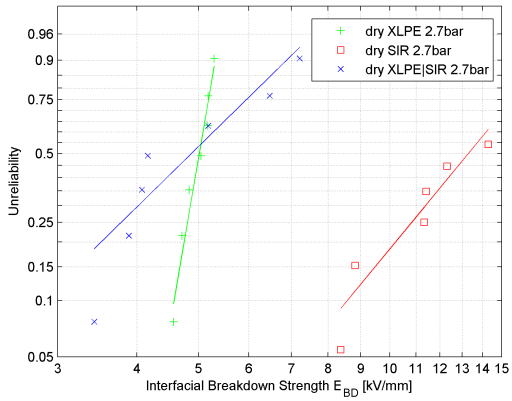

Figure 6.7: *Weibull plot of breakdown strength of dry XLPE|XLPE, SIR|SIR and XLPE|SIR interface with applied pressure of 2.7 bar.*

In this section a hybrid interface is examined. This interface is formed between a SIR and an XLPE sample. The applied pressure is set to 2.7 bar. This pressure was selected as the highest of the previously used pressure levels which is not deforming the SIR, i.e. the highest pressure level used in the SIR|SIR case. In Figure 6.7 the Weibull plot of the breakdown strength of the dry hybrid interface is shown in comparison with the equivalent XLPE|XLPE and SIR|SIR cases.

It is evident that using a dry combination of the two materials does not have any positive effect on the breakdown strength of the interface. Compared to the SIR|SIR interface, the hybrid has a substantially lower breakdown strength considering all the indices: minimum, mean and 63^{rd} percentile value. Compared to the XLPE|XLPE interface, the hybrid shows lower minimum and mean breakdown strength value and a greater measurement dispersion.

However an important note needs to be made regarding the XLPE|XLPE interface. Due to the low pressure (2.7 bar) applied, at the XLPE|XLPE case there is a suspicion that oil has flown in the interface increasing the breakdown strength. Therefore, in the absence of this oil leakage, the breakdown strength of the XLPE|XLPE would be lower. As a result, it can be argued that the breakdown strength of hybrid interface is slightly higher than of the XLPE|XLPE.

6.3 Breakdown strength of wet interface

6.3.1 XLPE|XLPE interface

In this section the results of the breakdown tests of wet XLPE|XLPE interface are presented. Two distinct pressure levels were examined: 5bar and 11.6 bar.

Figure 6.8 and Figure 6.9 present respectively the Weibull plot and the minimum, mean and 63^{rd} percentile values of the breakdown data gathered in this experiment. As it is seen and as it is expected, the presence of water in the interface has a detrimental effect on its breakdown strength. In the low pressure case (5 bar), the breakdown strength of the wet XLPE|XLPE interface is very low. All but one of the measurements were lower than the breakdown strength of air, showing that the wet XLPE|XLPE interface can be a very critical part of the insulation. When the pressure is increased to 11.6 bar, the breakdown strength is considerably increased as well. There is an agreement for this to all the three indices: minimum, mean and 63^{rd} percentile value. More specifically, for this pressure increase, which corresponds to 132% increase, there is an increase of 58% of the minimum, 68% of the mean and 68% of the 63^{rd} percentile breakdown strength value. Consequently, the positive effect of increasing pressure on the breakdown strength of wet XLPE|XLPE interface becomes evident. It can be argued that the higher pressure removes more water from the interface, bringing the behaviour of the interface closer to the dry case, i.e. increasing the breakdown strength.

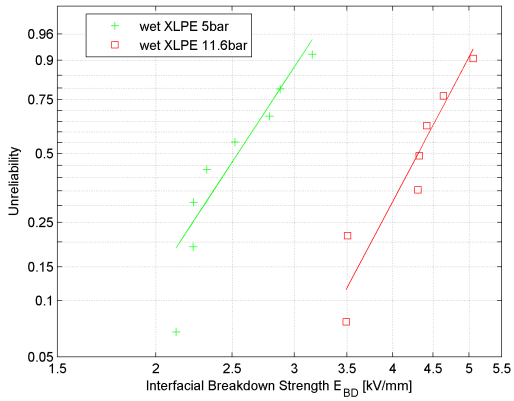

Figure 6.8: *Weibull plot of breakdown strength of wet XLPE|XLPE interface at two pressure levels (5 and 11.6 bar).*

6.3.2 SIR|SIR interface

In Figure 6.10, the behaviour of the wet interface formed by the softer SIR is examined. The wet SIR|SIR interface is tested under two pressure levels, 1.6 bar

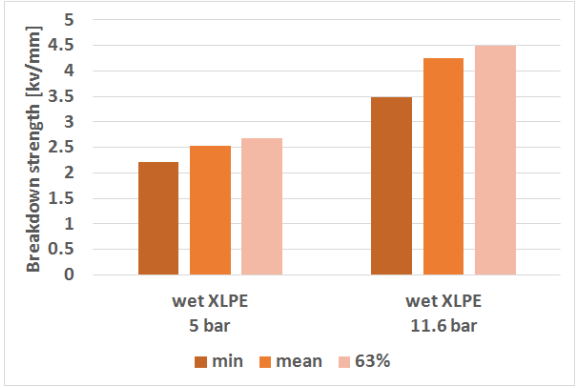

Figure 6.9: *Minimum, mean and 63^{rd} percentile breakdown strength of wet XLPE|XLPE interface (5 and 11.6 bar).*

and 2.7 bar. The negative impact of the water in the interface is here very evident. Most of the breakdown strength values recorded were lower than the one of air, with the lowest being under $2kV/mm$. Additionally, the pressure increase, from 1.6 bar to 2.7 bar, has a limited effect on the breakdown strength of the wet SIR|SIR interface. More specifically, for this pressure increase which corresponds to 69% increase, the mean breakdown strength increases only about 22%. As a result, it is seen that regardless the applied pressure, the wet SIR|SIR interface yields a very poor breakdown strength. As seen in Figure 6.11, all the three indices (minimum, mean and 63^{rd} percentile) agree and lead to the same conclusion.

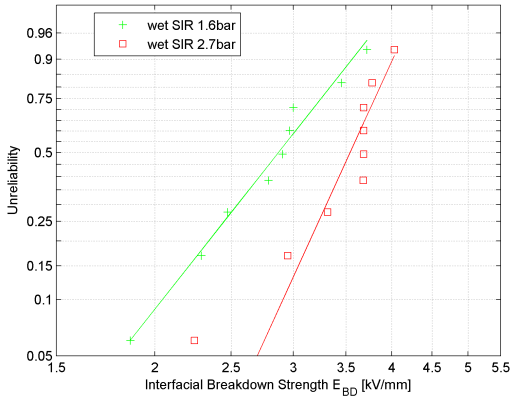

Figure 6.10: *Weibull plot of breakdown strength of wet SIR|SIR interface at two pressure levels.*

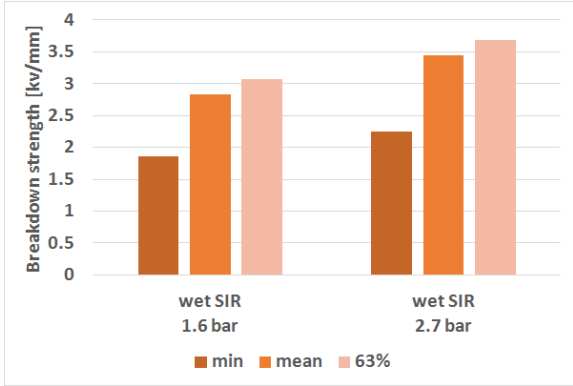

Figure 6.11: *Minimum, mean and 63^{rd} percentile breakdown strength of wet SIR|SIR interface (5 and 11.6 bar).*

6.3.3 Comparisons wet XLPEvsSIR

In Figure 6.12 the results of the wet XLPE|XLPE and wet SIR|SIR tests are shown, in comparison, on the same Weibull plot.

Comparing the behaviour of XLPE and SIR under wet conditions, it is noted that the breakdown strength of the XLPE|XLPE interface is relatively more sensitive - in terms of mean and 63^{rd} percentile value - to the pressure change than the SIR|SIR. However, in both cases the breakdown strength is very low, revealing the detrimental effect of water on the breakdown strength of the solid|solid interface.

By observing the plots, it is also noted that three out of the four minimum values are low (around 1.9 to 2.2 kV/mm) and very close to each other, regardless the material and the pressure. On the other hand, in the remaining plot, which corresponds to the wet XLPE|XLPE under the high pressure (11.6 bar), the minimum value is considerably higher (3.5 kV/mm). Considering the previous observation, the existence of a droplet of relatively large size in the void can be accused for the decreased breakdown strength. In the XLPE / 11.6 bar case, the applied pressure restricts the size of possible droplets, and therefore the strength is higher.

6.3.4 Hybrid wet interface

The last part of the wet interface experiments involves the hybrid interface, comprised by an XLPE and an SIR specimen which are held together under pressure of 2.7 bar. The Weibull plot of this experiment is shown in Figure 6.13 in comparison to the wet XLPE|XLPE / 5 bar and the wet SIR|SIR / 2.7 bar cases.

The combination of materials increases the breakdown strength of the interface safely above the strength of the air.Also, it allows a better breakdown strength despite the low pressure. Especially in comparison with the XLPE|XLPE case (5

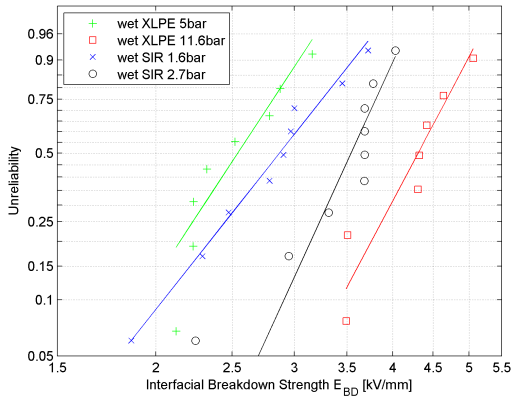

Figure 6.12: *Weibull plot of breakdown strength of wet XLPE|XLPE and SIR|SIR interface. Two different pressure levels for each material are shown.*

bar), the hybrid succeeds in achieving a breakdown strength comparable to SIR|SIR but in a much lower pressure (2.7 bar). Additionally, the use of hybrid interface increases considerably the minimum breakdown value. Even for the SIR|SIR case, where the mean value is comparable to the hybrid, the minimum value is very low. However, when replacing one of the specimens with XLPE (hybrid case) the minimum value increases substantially (see Figure 6.13).

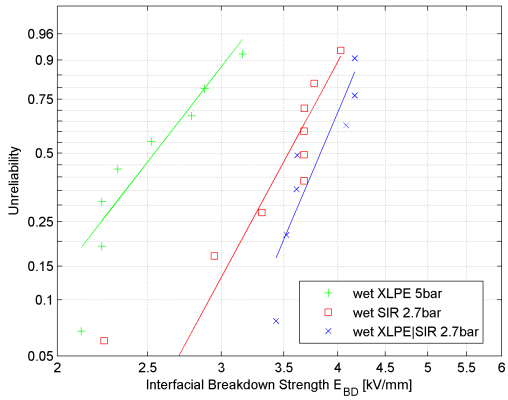

Figure 6.13: *Weibull plot of breakdown strength of wet XLPE|XLPE, SIR|SIR and XLPE|SIR interface (various pressure levels).*

In Figure 6.14 the wet hybrid case (2.7 bar) is compared to the XLPE|XLPE under two higher pressure levels (5 and 11.6 bar). The 2.7 bar hybrid interface has a comparable strength to the 11.6 bar XLPE|XLPE despite the enormous difference in the applied pressure (330% pressure increase). More specifically, in terms of

minimum value the two cases yield the same value and in terms of mean and 63^{rd} percentile the XLPE|XLPE performs only slightly better. Therefore, under wet conditions, the use of a combination of SIR and XLPE can arguably offer the breakdown strength of XLPE|XLPE but with much lower applied pressure. This comes in agreement with the observation that SIR is more water repellent than XLPE, in the sense that SIR helps in removing the water from the hybrid interface without the need of applying high pressure.

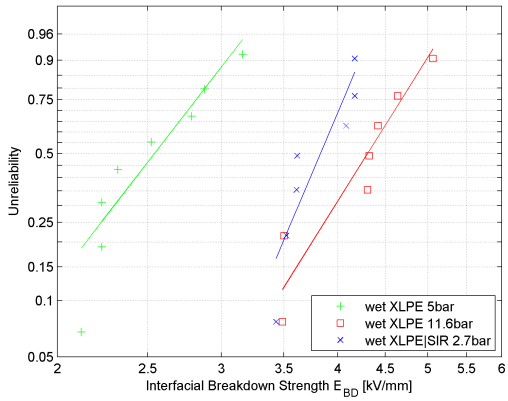

Figure 6.14: *Weibull plot of breakdown strength of wet XLPE|XLPE, SIR|SIR and XLPE|SIR interface (various pressure levels).*

6.4 Breakdown strength of lubricated interface

In this section, the breakdown strength of XLPE|XLPE, SIR|SIR and hybrid interface assembled with the oil is presented. Similarly to the wet interface case, the samples are momentarily immersed in insulating oil before they are mated. Following, the increasing voltage is applied and the breakdown voltage is recorded. After the necessary safety procedure, the samples were assessed and numbered according to the test procedure. The terms 'lubricated' and 'oily' are used here interchangeably and are used to describe the interface that is immersed in insulating oil before assembly.

As it is seen in Figure 6.15 the tests were performed for 5 bar and 11.6 bar XLPE|XLPE, 1.6 bar SIR|SIR and 2.7 bar XLPE|SIR. The case of SIR|SIR under pressure of 2.7 bar was also attempted, but the strength could not be measured as it will be explained further.

Evidently and as expected, the presence of oil in the interface results in high values of breakdown strength, especially in the SIR|SIR case. In some cases (high pressure XLPE|XLPE and SIR|SIR), the breakdown strength of the interface was so high that reached the limits of the experimental setup or the breakdown strength of the

material (SIR). This data is then recorded as singly censored data. Singly censored data are treated accordingly. When at least a few breakdowns happen along the interface they are put on the Weibull plot to be compared with the rest. In the case of SIR|SIR 2.7 bar, no breakdown occurred in the interface. Therefore, this case is not presented in Figure 6.15.

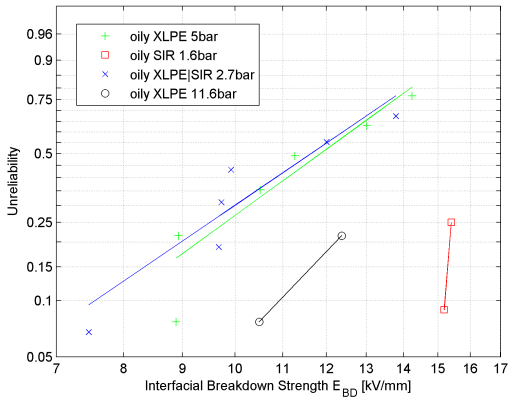

Figure 6.15: *Weibull plot of breakdown strength of oily XLPE|XLPE, SIR|SIR and XLPE|SIR interface.*

Furthermore, it is observed (Figure 6.15) that for the XLPE|XLPE 5 bar case, the breakdown values are very dispersed. Comparing the 5 bar with the 11.6 bar case, it can be argued that the 11.6 bar presents higher strength. This claim is possible considering the singly-censored data that occurred for the 11.6 bar case. However, the 2 measured 11.6 bar values are not higher than the 5 bar case. Therefore, it is unclear how significant the impact of pressure on lubricated XLPE|XLPE interface is.

When it comes to the lubricated SIR|SIR interface, only the 1.6 bar case could yield some measurements as it is mentioned earlier. Except the 2 measured values there were 5 more censored values. The censoring comes mostly by reaching the breakdown strength of the silicon rubber. This becomes obvious during the assessment of the specimen after the breakdown: there is a breakdown track through the material and not on the interface surface. In some cases there was no breakdown track. In these cases there was a surface breakdown, around the specimens. The characteristic of this type of breakdown is the much stronger flashing during the breakdown due to the fact that the channel is not through the material.

From the few measured values of lubricated SIR|SIR it is seen that despite the low applied pressure, there is a very high breakdown strength. It can be argued that this is because the interface cavities are filled with oil. However, this was the case for XLPE|XLPE as well, and the breakdown values were not equally high. As a result, it can be deduced that silicon rubber is the element that in combination with the oil increases significantly the breakdown strength.

Finally, the lubricated hybrid interface under pressure of 2.7 bar is examined. Its behaviour appears to be very similar to the behaviour of the lubricated 5 bar XLPE|XLPE interface, as seen in Figure 6.15. Considering that the silicon rubber behaves excellent with oil as seen previously - even in lower pressure levels, it is concluded that the XLPE is the weak element of the lubricated interface case. A possible explanation of the poor behaviour of XLPE is that, despite the presence of oil, air might be trapped in the cavities which leads to early breakdown.

In conclusion of the oiled interface case, it believed that the SIR in combination with oil is very promising, while the XLPE seems to not be particularly consistent. However, in order to extract safe conclusions, further investigation should be conducted to examine in particular the interaction of oil with the cavities formed on XLPE and SIR respectively.

6.5 Comparisons between the different interface conditions

In this section comparisons between the results for the different conditions (dry, wet, lubricated) are made in an attempt to clearly observe how the breakdown strength varies. First, the dry and wet case of XLPE and SIR for two pressure levels each are compared. Following, all three conditions are compared per interface material and per pressure level.

6.5.1 Dry vs wet interface

XLPE|XLPE interface

Figure 6.16 presents the Weibull plot of the breakdown values of dry and wet XLPE|XLPE interface under pressure of 5 bar and 11.6 bar. As it is seen the effect of water on the interface is more significant at the 5 bar case. More specifically, at 5 bar the breakdown strength of the dry interface is 75% increased compared to the wet. In contrast, the respective increase for the 11.6 bar case is only 21%. This result supports the hypothesis that, for wet interface, higher applied pressure forces the water out of the interface leading to a breakdown strength similar to the dry case.

In Figure 6.17 the minimum, mean and 63^{rd} percentile of the test results of Figure 6.16 are shown together. As it is observed, there is an adequate agreement of all the indices.

SIR|SIR interface

Through Figure 6.18 a comparison between the dry and wet SIR|SIR interface under two pressure levers is possible. As it is seen, there is an undeniable increase

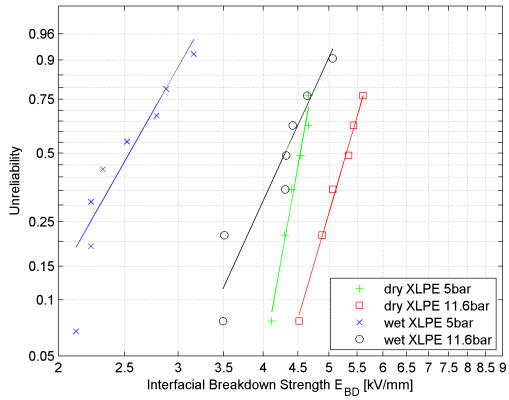

Figure 6.16: *Weibull plot of breakdown strength of dry vs wet XLPE|XLPE interface at two pressure levels.*

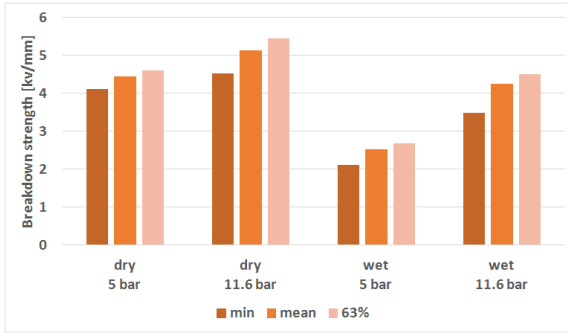

Figure 6.17: *Minimum, mean and 63^{rd} percentile breakdown strength of dry vs wet XLPE|XLPE interface (two pressure levels for each condition).*

on the breakdown strength when moving from wet to dry interface. The highest value of the wet case is lower from the lower value for the dry case regardless the applied pressure. Evidently, wet SIR has low breakdown strength even with high applied pressure.

For silicon rubber, the influence of water is quite high regardless the pressure level. From wet to dry interface there is a 180% increase of the breakdown strength for 1.6 bar and 221% increase for 2.7 bar. As seen in Figure 6.19, the minimum, mean and 63^{th} percentile values all describe the change in a similar way.

In conclusion, SIR|SIR interface shows a higher increase than XLPE|XLPE when going from wet to dry conditions. This is partially because SIR behaves very poor when wet and partially because XLPE seems to be a worse interfacial material. Even though XLPE cannot achieve the high strength of dry SIR, it is more consistent in the sense that the wet and dry condition breakdown values are closer and

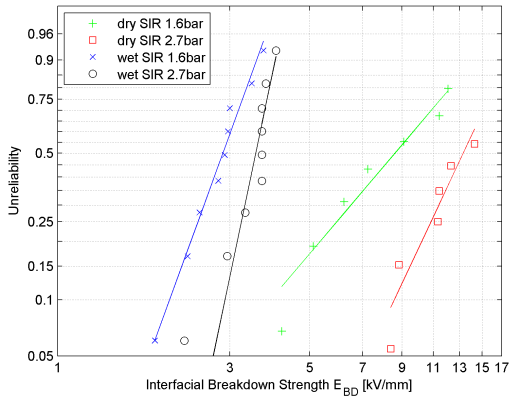

Figure 6.18: *Weibull plot of breakdown strength of dry vs wet SIR|SIR interface at two pressure levels.*

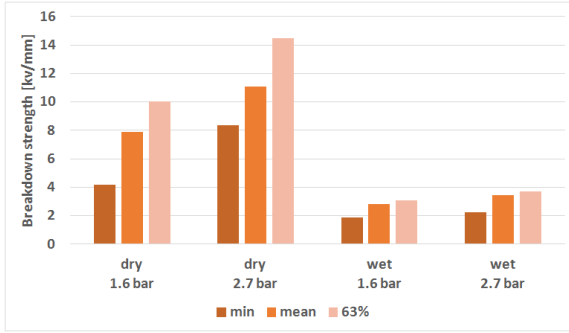

Figure 6.19: *Minimum, mean and* 63^{rd} *percentile breakdown strength of dry vs wet SIR|SIR interface (two pressure levels for each condition).*

not so dispersed.

6.5.2 Dry vs Wet vs Lubricated

In this section the results are presented for comparison in graphs with only variable the interface condition i.e. dry, wet, lubricated. The four cases are: XLPE|XLPE 5 bar, XLPE|XLPE 11.6 bar, SIR|SIR 1.6 bar and XLPE|SIR 2.7 bar.

XLPE|XLPE

First, the 5 bar XLPE|XLPE interface is examined. As it is seen in Figure 6.20 and Figure 6.21, there is a clear difference between the three conditions. Taking

the dry case as a reference, the breakdown strength decreases when the interface is wet and increases when the interface is lubricated. More specifically, from dry to wet interface there is a decrease of 48% of the minimum, 43% of the mean and 42% of the 63^{rd} percentile value. Accordingly, from dry to lubricated, there is an increase of 116%, 150% and 178% respectively.

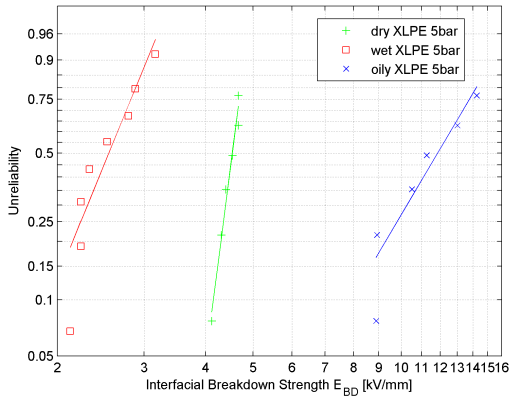

Figure 6.20: *Weibull plot of breakdown strength of dry vs wet vs lubricated XLPE|XLPE interface at 5 bar.*

The agreement between all three indices is notable and it shows that any of them could be used to assess the breakdown strength of XLPE|XLPE interfaces.

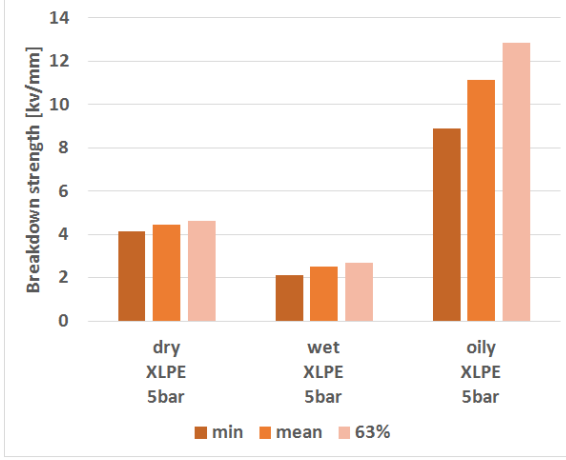

Figure 6.21: *Minimum, mean and 63^{rd} percentile breakdown strength of dry vs wet vs lubricated XLPE|XLPE interface at 5 bar.*

In the same manner, the 11.6 bar XLPE|XLPE case is depicted in Figure 6.22 and Figure 6.23. In the lubricated case, there are only two measurements due to the

limitations of the setup, as it is mentioned before.

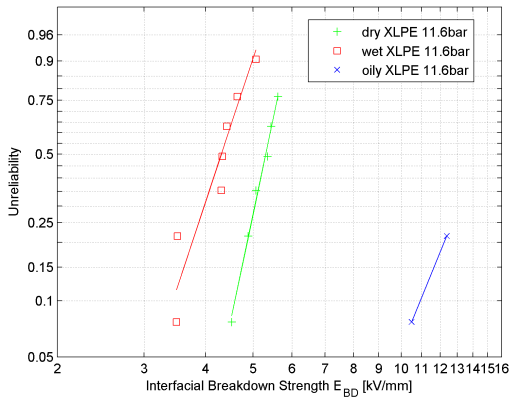

Figure 6.22: *Weibull plot of breakdown strength of dry vs wet vs lubricated XLPE|XLPE interface at 11.6 bar.*

Again, there is a decrease of the breakdown strength between dry and wet interface and a considerable increase between dry and lubricated. The decrease corresponds to 22% of the minimum, 17% of the mean and 17% of the 63^{rd} percentile value. On the other hand, the increase is 132% for the minimum and 122%for the mean. The 63^{rd} percentile value for the lubricated case is not considered due to the low number of measurements. One more time, the agreement of the indices in showing the change trend is notable.

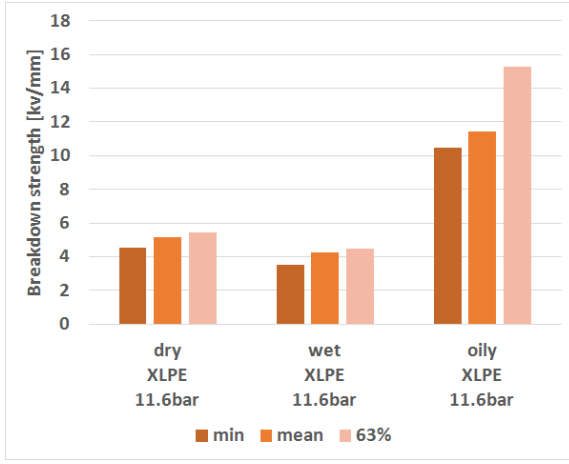

Figure 6.23: *Minimum, mean and 63^{rd} percentile breakdown strength of dry vs wet vs lubricated XLPE|XLPE interface at 11.6 bar.*

SIR|SIR interface

Figure 6.24 and Figure 6.25 put the 1.6 bar SIR|SIR different interface conditions under comparison in terms of Weibull plot and the three indices respectively. Similarly to the XLPE cases and as expected, the presence of water lowers the breakdown strength and the presence of oil in the interface increases it (in comparison to the dry interface). For the case where oil is in the interface, most of the experiments led to a breakdown voltage which was high enough to break the silicon rubber itself before the interface. Therefore, only two measured values are seen in Figure 6.24.

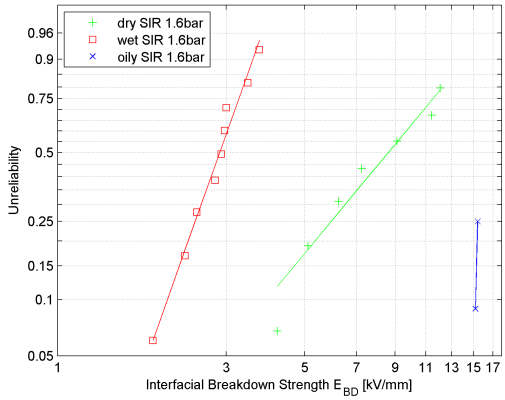

Figure 6.24: *Weibull plot of breakdown strength of dry vs wet vs lubricated SIR|SIR interface at 1.6 bar.*

Comparing the dry interface with the wet, it seems that water causes a substantial decrease of the breakdown strength. The decrease is different for each index but of the same order: 56% for the minimum, 64% for the mean and 70% for the 63^{rd} percentile value. On the other hand, there is a considerable difference in the indices when moving from dry to lubricated interface. The increase is 263% for the minimum value and 93% for the mean (the 63^{th} percentile is not considered due to inadequate number of measurements). This divergence between the change of the minimum and the mean value is due to the large dispersion of the breakdown strength values of the dry SIR|SIR interface.

Hybrid interface

Finally, in Figure 6.26 the Weibull plot for the breakdown strength of the hybrid interface under the three conditions is presented. As in the previous cases, there is a notable increase of the breakdown strength when moving from wet to lubricated interface. All the indices agree: there is a 118% increase for the minimum, 112% for the mean and 132% for the 63^{rd} percentile value.

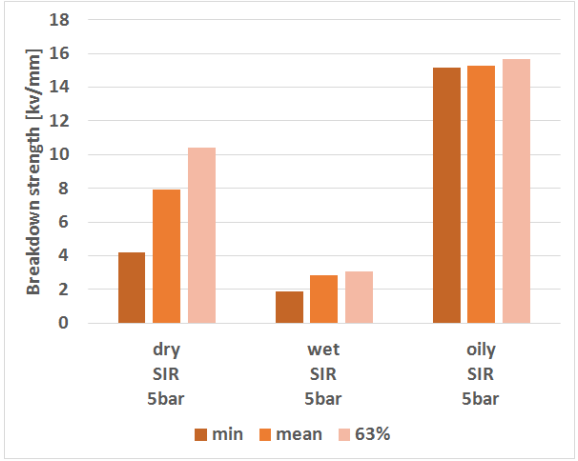

Figure 6.25: *Minimum, mean and 63^{rd} percentile breakdown strength of dry vs wet vs lubricated SIR|SIR interface at 1.6 bar.*

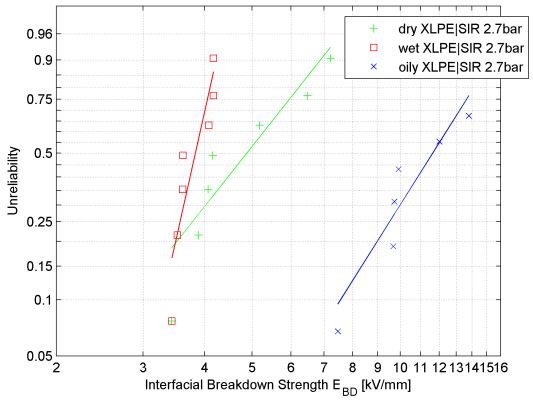

Figure 6.26: *Weibull plot of breakdown strength of dry vs wet vs lubricated XLPE|SIR interface at 2.7 bar.*

However, when comparing the dry and the wet case the it is seen that the behaviour of the hybrid interface is not the same as for the XLPE|XLPE and SIR|SIR. The breakdown strength of the interface barely decreases when wet. More specifically, there is no decrease of the minimum value, 22% decrease for the mean and 26% for the 63^{rd} percentile value. Even though the breakdown strength of the dry hybrid interface is not as high as the strength of XLPE|XLPE or SIR|SIR, the fact that it is not heavily affected by the presence of water can be of value. It can be argued that the combination of XLPE and SIR creates an interface which combines the positive characteristics of both materials and achieves comparable breakdown strength in much lower pressure (in comparison with XLPE|XLPE). The fact that

the minimum breakdown value does not get lower when the interface is wet shows that the hybrid interface could be a considerate choice in applications where water might be present.

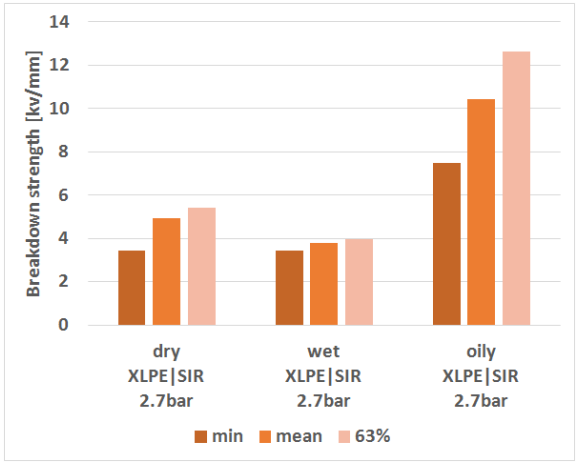

Figure 6.27: *Minimum, mean and 63^{rd} percentile breakdown strength of dry vs wet vs lubricated XLPE|SIR interface at 2.7 bar.*

The four above cases (XLPE|XLPE 5 bar, XLPE|XLPE 11.6 bar, SIR|SIR 1.6 bar and XLPE|SIR 2.7 bar) evidently show that as a rule the breakdown strength of a wet interface is worse compared to the dry, when all other parameters (pressure, materials involved) are held constant. Also, the positive influence of oil in the interfacial breakdown strength is unquestionable and leads to the suggestion that oil could be used on the mating surfaces to improve their breakdown strength.

6.6 Interfacial breakdown tracking

The test samples that were used for the experimental determination of the breakdown strength of the various interfaces are also a valuable source of information themselves. The energy (heat) released during the electrical breakdown resulted in permanent paths (tracks) on the interfacial surface of the specimens. These tracks are unique for each pair of samples - they are a form of "fingerprint". However, specific patterns or repeated characteristics of these tracks were observed for each

material and/or interface condition. This section presents the most characteristic breakdown track examples of each interfacial condition (dry, wet, lubricated) and material combination (XLPE|XLPE¡ SIR|SIR and hybrid). Comments are made upon the findings and some reasoning is attempted. The samples were magnified using an optical microscope and the images were captured with an embedded to the microscope digital camera.

6.6.1 Dry interface

XLPE|XLPE interface

The dry XLPE samples are characterised by a clear and clean breakdown path and tree-like incomplete breakdown channels in both sides starting from the edges (Figure 6.28a and 6.28b). Also, there is substantial burning marks along a wide part of the interface. The heat evidently caused melting of the material and subsequently the specimens were attached after removal from the test setup.

The tree-like channels on the interface can be explained by the partial discharge activity which was also noticed during the experiments in the form of audible discharges. These partial discharges initiated and grew the channels in a way that reminds both electrical trees and surface tacking paths. The presence of air cavities that enhance the field close to the edge of the interface justifies this behaviour.

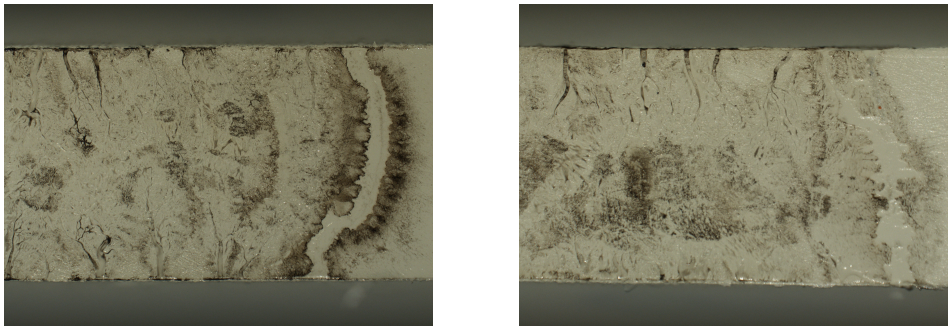

(a) 5 bar (b) 11.6 bar

Figure 6.28: *Breakdown tracks of dry XLPE|XLPE interface*

In Figure 6.29, a characteristic breakdown path of the low pressure (2.7 bar) case of dry XLPE|XLPE interface is shown. This breakdown path appears quite different compared to the other (higher pressure) cases. It actually appears to be more similar to the lubricated interface case (see Figure 6.36). This supports the suspicion (subsection 6.2.1) that oil leaked in the interface due to the low applied pressure.

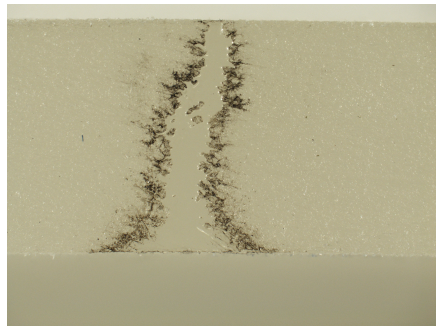

Figure 6.29: *Breakdown track of low pressure dry XLPE—XLPE interface*

SIR|SIR interface

The dry SIR|SIR interface has a very different appearance. In the majority of the samples, one, heavily burnt breakdown path was observed (Figure 6.30). There were no branches or secondary paths implying that the interface withstands the voltage without obvious permanent damage - until it breaks down. Among the tests, no systematic differences between the different pressure levels were observed. After the breakdown, the specimens were not attached which means that the released heat does not cause significant melting of the material. The black regions on the sides of the breakdown path can be attributed to the smoke that iss being axhausted during the breakdown.

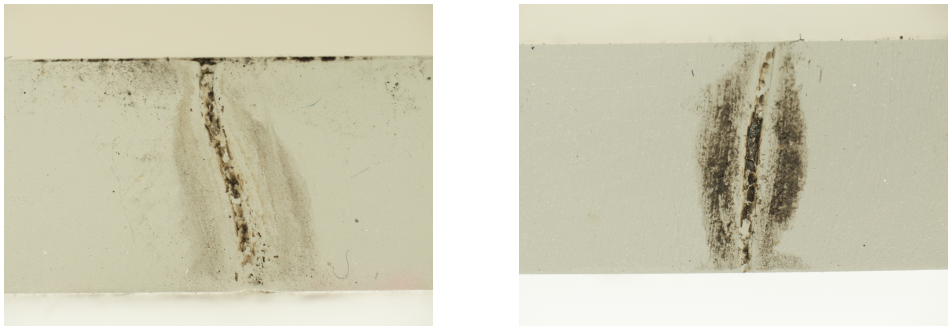

(a) 1.6 bar (b) 2.7 bar

Figure 6.30: *Breakdown tracks of dry SIR|SIR interface*

Hybrid interface

Two representative breakdown paths on the XLPE side of the hybrid interface are shown in Figure 6.31. The combination of two materials increases the uncertainty of

any comments on the breakdown tracks and, therefore, Figure 6.31 is only included for completeness.

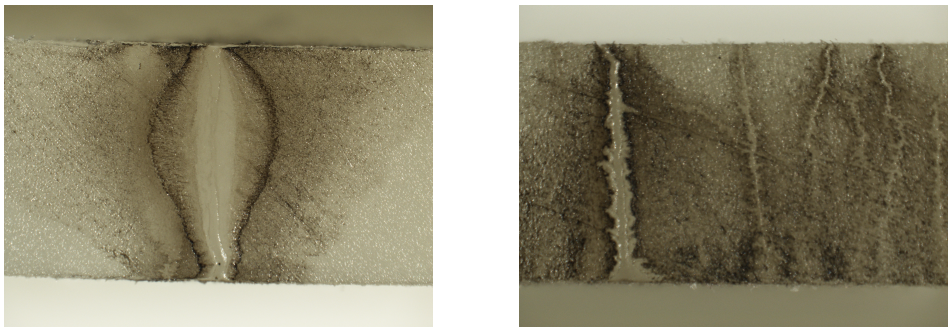

(a) (b)

Figure 6.31: *Breakdown tracks of dry hybrid interface*

6.6.2 Wet interface

XLPE|XLPE interface

The presence of water in the interface has a considerable effect in the appearance of the samples. Despite the low applied field (compared to the dry case the wet has a much lower strength) there is very evident pre-breakdown activity. This discharge activity is seen on the interfaces in the form of electrical tree-like tracks in all the length of the specimens (Figure 6.32 and Figure 6.33). The extensive pre-breakdown activity was visible and audible during the tests.

Regarding the main breakdown paths, as in the case of dry XLPE, they are clear and clean i.e. there is no burnt residue material in the channel. Therefore, it is seen that despite the water, the material still experiences heavy, instant melting during the breakdown which results in this appearance.

SIR|SIR interface

In a similar manner, for the wet SIR|SIR interface, except of the main breakdown path there are more discharge paths along the surface Figure 6.34. Due to the lower voltage at breakdown, the burning of the material is not so extended as in the dry case. In most cases a clear main breakdown path was observed. In addition to this, incomplete tree-like tracks beginning from both edges of the specimens were also noticed. These tree-like tracks are attributed to the presence of water which enhance the initiation of partial discharges.

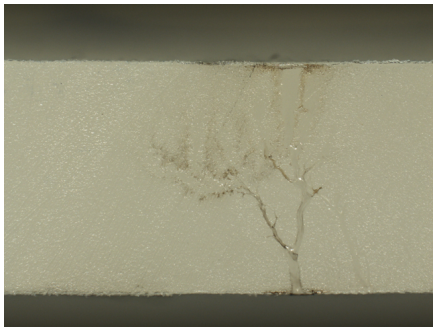

(a)

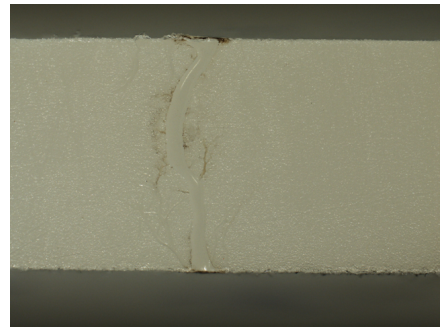

(b)

Figure 6.32: *Breakdown tracks of wet XLPE|XLPE interface (5 bar)*

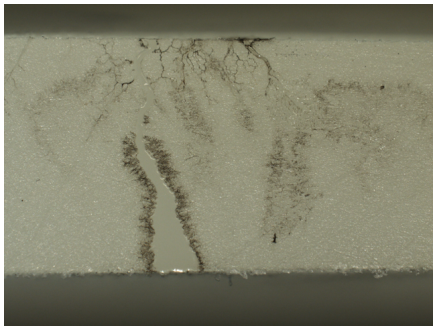

(a)

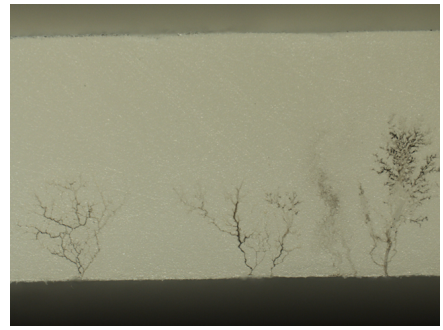

(b)

Figure 6.33: *Breakdown tracks of wet XLPE|XLPE interface (11.6 bar)*

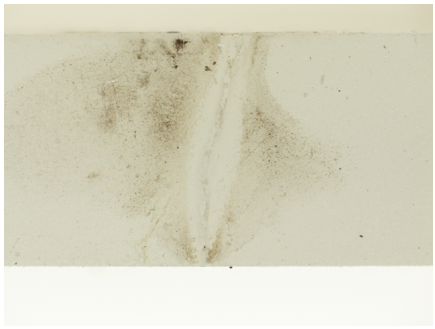

(a)

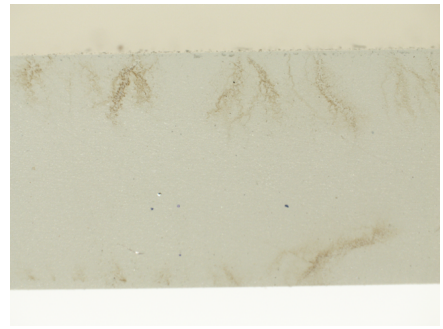

(b)

Figure 6.34: *Breakdown tracks of wet SIR|SIR interface*

Hybrid interface

In Figure 6.35 the XLPE (6.35a) and the SIR (6.35b) side of the wet hybrid interface is shown. This set of specimens is selected in order to highlight the difference between the XLPE and SIR samples in terms of the breakdown tracks. As it is seen, the main path is clean on the XLPE side, while it is heavily burnt for the SIR side. This behaviour is attributed to the different materials and it was common among the test samples, regardless the condition of the interface (dry, wet, lubricated).

(a) (b)

Figure 6.35: *Breakdown tracks of wet hybrid interface. Both the XLPE (a) and SIR (b) sides of the interface are shown for comparison.*

6.6.3 Lubricated interface

XLPE|XLPE interface

The characteristic breakdown track for the lubricated XLPE|XLPE interface is shown in Figure 6.36a and 6.36b for the 5 and 11.6 bar case respectively. It is a clean, smooth path which is obviously created by local melting of the material. The fact that there is no tree-like tracks or burning marks implies that the oil restricts the pre-breakdown activity. Therefore, even though higher a field strength is reached, the surface of the specimens is not impaired - except, of course, from the breakdown path. As a result, it can be argued that the presence of oil in the interface improves not only the breakdown strength but also the overall performance of the interface, since no permanent damage occurs from any pre-breakdown activity.

SIR|SIR interface

The lubricated SIR|SIR breakdown path shows a remarkable similarity to the dry case (Figure 6.37). Again, one heavily burnt breakdown path prevails. The only

(a) 5 bar (b) 11.6 bar

Figure 6.36: *Breakdown tracks of lubricated XLPE|XLPE interface*

difference that can be noted is that the burning marks are confined only in the immediate vicinity of the breakdown path.

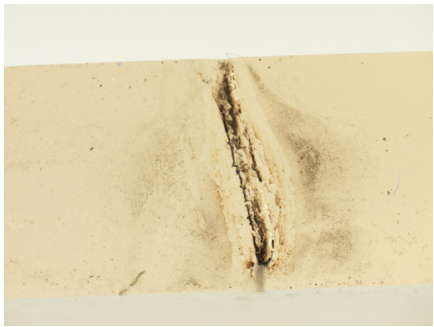

Figure 6.37: *Breakdown tracks of lubricated SIR|SIR interface*

Hybrid interface

Finally, in Figure 6.38 the breakdown track of the lubricated hybrid interface is seen. The XLPE side and part of the SIR side are shown. One more time the difference between the tracks on XLPE and SIR is highlighted: the XLPE melts and creates a clean path while the SIR burns.

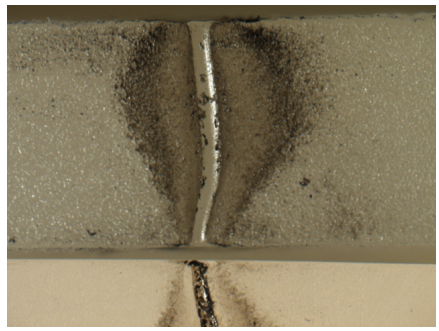

Figure 6.38: *Breakdown tracks of lubricated hybrid interface. The XLPE and partially the SIR sides of the interface are shown for comparison.*

Chapter 7

Discussion and Conclusions

In this section all the significant qualitative conclusions of this work are presented in a direct and concise way. The conclusions are arranged and organised and discussed as a response to the research questions posed in section 1.4.

According to the contact theory (section 3.2) increasing the applied pressure on a given dry-mated solid|solid interface leads to a higher breakdown strength. This dependency has been shown experimentally for XLPE|XLPE interfaces ([19]) and in the current work it is confirmed by repeating the tests. Furthermore, the same dependence is experimentally confirmed for an interface formed by a softer material. The 50Hz/AC breakdown strength of a dry-mated SIR|SIR interface shows an even higher relative increase with increasing applied pressure.

By extending the contact theory, the impact of varying the material elasticity modulus on the breakdown strength is shown. Specifically, in this work, it is theoretically demonstrated that an interface formed by softer materials will have a higher breakdown strength. This claim is experimentally confirmed by testing dry-mated XLPE|XLPE and SIR|SIR interfaces. The more elastic material (SIR|SIR interface) is shown to sustain higher breakdown strength, even in cases that the applied pressure is considerably lower. However, the breakdown data of the dry-mated SIR|SIR show a wider dispersion, which is not implied by the theoretical model. Possibly, this behaviour is related to some other trait of the silicon rubber as a material or to the lower pressure values. Further investigation on the underlying mechanisms is suggested.

The case in which an XLPE and a SIR sample are mated in air to form a hybrid interface is experimentally shown that has no obvious positive effect on the breakdown strength. Specifically, the dry hybrid interface performs similarly to the XLPE|XLPE case while the strength of SIR|SIR is clearly higher.

The presence of water in the interface is experimentally shown that has in any case a detrimental effect on the breakdown strength of the interface. In comparison, the SIR|SIR wet-mate interface behaved worse than the respective XLPE|XLPE, both in terms of dielectric strength and relative pressure dependency. In most cases, the breakdown strength of the interface falls lower than the breakdown strength of the standard air. This poor behaviour is explained by the assumption of sizable water droplets captured in the interfacial cavities which cause local field enhancement and trigger tree-like tracking and eventually the breakdown. Furthermore, it is observed that higher applied pressure has a sizable positive effect only in the XLPE|XLPE case. This observation supports the assumption of water droplets in the interface, in the sense that higher pressure forces the water out of the interface which leads to improved strength. However, the fact that increased pressure does not particularly improve the SIR|SIR case implies that in the presence of water the SIR is, as a material, more sensitive in terms of breakdown strength.

A remarkable observation is made with regard to the wet-mate hybrid interface. A relatively good breakdown strength, comparable to the strength of the high pressure XLPE|XLPE, is achieved despite the low applied pressure. This leads to the suggestion that the hybrid interface - under wet conditions - combines the beneficial traits of the two materials and it can provide a higher strength with low applied pressure.

Between the dry and wet case there is a higher relative difference for SIR|SIR rather than for XLPE|XLPE interface. The latter, even though it shows low breakdown strength, seems to be more consistent and less affected from the presence of water; especially when the applied pressure is higher.

The superiority of the lubricated (oily) interface - regardless the material - is undoubtedly shown through experimental testing. Especially the SIR|SIR interface shows exceptional performance as in some cases the interfacial strength exceeds the dielectric strength of the material. The hypothesis is made that the insulating oil fills the cavities in the interface and therefore the breakdown strength increases. Some of the cavities are thought to trap air and therefore relatively small differences occur between the materials and the pressure levels. This hypothesis supports the argument that the air-filled cavities are indeed the determining parameter for the breakdown. As a result, it is suggested that in practical applications which include solid|solid interfaces, some insulating lubricant should be applied in the interface to ensure a higher breakdown strength.

The breakdown data are generally presented in a Weibull plot and represented by the 63^{rd} percentile value. In this work, all the results were represented also by the minimum and mean value. It was observed that - with very few exceptions - the qualitative comparison of different cases is possible with the minimum or the mean value. This observation could be of value when large amount of cases need to be compared in a fast, qualitative way.

Observation of the test samples with a microscope after breakdown, offers a degree of insight about their behaviour. Tree-like tracking on the contact surface

of the samples reveals pre-breakdown activity. This activity fits with the concept of cavity induced breakdown supported by the contact theory. Especially for the XLPE|XLPE case, the tree-like tracks are more evident than for SIR|SIR. This is attributed in the material and it implies that SIR shows better mating quality. The presence of water makes the pre-breakdown activity more evident and in lower voltages. On the other hand, the oil seems to fill the cavities and diminish the pre-breakdown activity. This is supported by the fact that, except the main path, there were found no other tracking marks on the lubricated interfaces. In any case, the study of the breakdown tracks in this work is considered basic, and further work on the subject is suggested.

Future work

The study of solid|solid interfaces has a great potential for further investigation both in theoretical and in experimental way.

First, the above results can be verified with other materials with different elasticity. Achieving similar test results with other material that agree to the theoretical approach, will erase any doubt on its validity. Regarding the breakdown tracks, it is evident that further and more systematic observation could result in usable insight and cocnlusions.

The theoretical model should also be quantitatively verified. This would require surface roughness measurements, so that the breakdown strength is calculated. Further, the model can be extended and developed in order to include impact of water and oil in the interface.

A field with enormous potential is the simulation of the breakdown of solid|solid interfaces. A study on finite element modelling and simulation of the contact surface could provide substantial insight on the interfacial breakdown mechanisms. However, this task is considered very complicated due to the many parameters involved, especially when it comes to breakdown triggering.

Another approach to the issue of solid|solid interface strength is the study of the partial discharge initiation voltage, instead of the breakdown strength directly. The electrical breakdown in the interface can be considered a complicated, stochastic phenomenon affected by many parameters. On the other hand, the partial discharge initiation might be less stochastic and more systematic process. Some investigation in this direction has been performed in [20], but there is absolutely more work to be done.

Finally, the behaviour of solid|solid interfaces under DC and low frequency AC should be explored. Since more and more applications switch to DC or low frequency AC, the potential of solid|solid interfaces in these conditions should be assessed.

Bibliography

[1] S. Midttveit, B. Monsen, S. Frydenlund, K. Stenevik, "Subsea Power Systems - a Key Enabler for Subsea Processing", OTC paper 20621, Offshore Technology Conference, Houston, Texas, USA, 3-6 May 2010

[2] P. Weiss, S. Beurthey, Y. Chardard, J.-F. Dhedin, T. Andre, K. Rabushka, C. Tourcher, F. Gauch, C. Micoli, "Novel wet-mate connectors for high voltage and power transmissions of ocean renewable energy systems", 4th International Conference on Ocean Energy 2012, Oct 2012, Dublin, Ireland

[3] "High Voltage Subsea Connection," SINTEF project, https://www.sintef.no/en/projects/subsea-power-supply/

[4] Jon Thore Myklatun, "Condition Monitoring of Subsea Connectors", Maste thesis, Norwegian University of Science and Technology (NTNU), Department of Electric Power Engineering, June 2014

[5] Siemens SpecTRON Subsea Medium and High Power Electrical Connector Systems brochure, http://www.energy.siemens.com/

[6] MacArtney Underwater Technology, GreenLink Wetmate 11kV, http://macartney.com/systems/connectivity/greenlink/greenlink-wetmate-11kv

[7] First Subsea, "Cable connectors for Phase 2 Fukushima Floating Wind Farm", newsletter, 6 January 2015

[8] SINTEF website, Project description, http://www.sintef.no/projectweb/subseapowersupply/

[9] D. Fournier and L. Lamarre, "Effect of Pressure and Length on Interfacial Breakdown Between Two Dielectric Surfaces,"Proceedings of the IEEE International. Symposium on Electrical Insulation, Baltimore, MD, June 1992, pp. 270-272 © 1992 IEEE

[10] D. Fournier and L. Lamarre, "Interfacial Breakdown Between Two EPDM Surfaces," Proceedings of the IEE Sixth International Conference on Dielectric Materials, Measurements and Applications, Manchester, U.K., September 1992, pp. 330-333, © 1992 IEEE

[11] D. Fournier and L. Lamarre, "Effect of Pressure and Temperature on Interfacial Breakdown Between Two Dielectric Surfaces, " Proceedings of the IEEE Conference on Electrical Insulation and Dielectric Phenomena, Victoria, B.C., October 1992, pp. 229-235, © 1992 IEEE

[12] D. Fournier, C. Dand and L. Paquin, "Interfacial Breakdown in Cable Joints," Proceedings of the IEEE International. Symposium on Electrical Insulation, Pittsburgh, PA, June 1994, pp. 450-452, © 1994 IEEE

[13] D. Fournier, "Effect of the surface roughness on interfacial breakdown between two dielectric surfaces," Conference Record of the 1996 IEEE International Symposium on Electrical Insulation, 16-19 Jun 1996, © 1996 IEEE

[14] C. Dand and D. Fournier, "Dielectric Performance of Interfaces in Premolded Joints," IEEE Transactions on Power Delivery, Jan 1997, © 1997 IEEE

[15] Technical data sheet for ELASTOSIL®LR 3003/60 A/B, Version: 1.13, Date of last alteration: 18.05.2012, WACKER SILICONES

[16] Wilson, M.P.; Given, M.J.; Timoshkin, I.V.; MacGregor, S.J.; Wang, T.; Sinclair, M.A.; Thomas, K.J.; Lehr, J.M., "Weibull statistical analysis of impulse-driven surface breakdown data," Pulsed Power Conference (PPC), IEEE, 19-23 June 2011, © 2011 IEEE

[17] Standard Test Method for Dielectric Breakdown Voltage and Dielectric Strength of Solid Electrical Insulating Materials at Commercial Power Frequencies, ASTM D149 - 09(2013)

[18] M. Hasheminezhad, E. Ildstad, and A. Nysveen, Breakdown strength of solid-solid interface, in Solid Dielectrics (ICSD), 2010 10th IEEE International Conference on, Jul. 2010, pp. 14, © 2010 IEEE

[19] Hasheminezhad, S.M., "Breakdown strength of solid solid interfaces", PowerTech, 2011 IEEE Trondheim, vol., no., pp.17, 19-23 June 2011, © 2011 IEEE

[20] M. Hasheminezhad and E. Ildstad, Partial discharge inception of interface voids versus mechanical surface pressure, in High Voltage Engineering and Application (ICHVE), 2010 International Conference on, Oct. 2010, pp. 397 400.

[21] Hasheminezhad, M.; Ildstad, E.. "Application of contact analysis on evaluation of breakdown strength and PD inception field strength of solid-solid interfaces," Dielectrics and Electrical Insulation, IEEE Transactions on, February 2012, © 2012 IEEE

[22] B. Bhushan, "Analysis of the real area of contact between a polymeric magnetic medium and a rigid surface," ASME Journal of Tribology, vol. 106, pp. 26-34, 1984

[23] Hao Chen; Johnson, M.H.; Aliprantis, D.C., "Low-Frequency AC Transmission for Offshore Wind Power", IEEE Transactions on Power Delivery, IEEE, Oct. 2013, © 2013 IEEE

[24] Stone, G.C. ; Ontario Hydro, Toronto, Ontario ; van Heeswijk, R.G., "Parameter Estimation for the Weibull Distribution", Electrical Insulation, IEEE Transactions on (Volume:EI-12 , Issue: 4), Aug. 1977, © 1977 IEEE

[25] N. R. Mann, R. E. Schafer, N.D. Singpurwalla, "Methods for Statistical Analysis of Reliability and Life Data", John Wiley and Sons, 1974

[26] W. Q. Meeker, W. Nelson, "Weibull Percentile Estimates and Confidence Limits from Singly Censored Data by Maximum Likelihood," IEEE Trans Reliability, Vol R-25, Apr 1976, © 1976 IEEE

[27] Askeland, Donald R.; Phul, Pradeep P., "The science and engineering of materials (5th ed.)." Cengage Learning, 2006

[28] AZO materials, http://www.azom.com/properties.aspx?ArticleID=920

[29] E. Kantar, D Panagiotopoulos, "Impact of Contact Pressure on Breakdown Strength of Solid-Solid Interfaces," 24^{th} Nordic Insulation Symposium on Materials, Components and Diagnostics, Copenhagen, 15 – 17 June, 2015

[30] IEC/IEEE Guide for the Statistical Analysis of Electrical Insulation Breakdown Data (Adoption of IEEE Std 930-2004), © 2007 IEEE

[31] F.H. Kreuger, "Industrial High Voltage Vol. II", Delft University Press, 1992

[32] Erling Ildstad, TET4160 High Voltage Insulation Materials, Compendium, NTNU, August 2014

[33] F.H. Kreuger, "Industrial High Voltage Vol. I", Delft University Press, 1992

[34] MIDEL®7131, Dielectric Insulating Fluid Overview (datasheet), MIDEL, September 2014

[35] N.G. Trinh, "Electrode Design for Testing in Uniform Field Gaps", Power Apparatus and Systems, IEEE Transactions on (Volume:PAS-99 , Issue:3, p. 1235 - 1242), May 1980, © 1980 IEEE

[36] R. Arora, W. Mosch, "High voltage insulation engineering: behaviour of dielectrics, their properties and applications", New Age International, Jan 1, 1995

[37] TET4160 High Voltage Insulation Materials, course material, NTNU

[38] Finite Element Method Magnetics software, David Meeker, http://www.femm.info/

[39] STRUERS Abramin Microprocessor controlled table top machine for automatic grinding, lapping and polishing of all materials manual, http://www.struers.com/default.asp?doc_id=371

Appendix A

Weibull code

This Matlab function code was developed for the Weibull parameter calculation and the Weibull plot plotting of singly censored data according to [30].

```
%% Estimation of Weibull parameters and Weibull plotting of SINGLY cencored
data (according to IEEE guide for the statistcal analysis of electrical
insulation breakdown data - Std 930 2004)
% data: all BD values (unsorted)
% n:    total number of specimens/tests (length of cencored data)
% m: if m=1, White method is used
% m: if m=2, simple regression method is used

function [u63,beta,R]=myWBLplot(data,n,l,k,xmin,step,xmax,m) % input: (BD
data,total no of tests,LineSpec for data(string), LineSpec for fitted
line(string),xmin,step,xmax,method)

r=length(data); % the number of specimens that broke down
for n0=1:r % calculate the probability
    P(n0)=(n0-0.44)/(n+0.25);
end
x=sort(data);

% calculate correlation for goodness of fit
matrix=corrcoef(log(x),log(-log(1-P)));
R=matrix(1,2); % for verdict see figure A.8 IEEE guide

figure(2)% WBL plot
x=log(x);
y= log(-log(1-P));
plot(x, y,l) % plot data. If it is a straigt line if data fit
hold on
```

```
if m==1
    [beta,u63]=weightedregression(data,n);
    p=[beta  -log(u63)*beta];
    y=polyval(p,x);
    plot(x,y,k); % plot the fitted line
elseif m==2
    p=polyfit(x,y,1); % fit a line (linear regression - least squares)
    y=polyval(p,x);
    plot(x,y,k); % plot the fitted line
    beta=p(1);
    u63=exp((0-p(2))/p(1)); % 63% @ log(-log(1-0.632))=0
end
figure(2)
% x axis
xx=(xmin:step:xmax); % all data expected to be in this range
set(gca,'XLim',[log(xmin) log(xmax)]);% this changes the axis limits
D=log(xx);
set(gca,'XTick',D);% defines which ticks are shown but does not change the
axis
C=strsplit(num2str(exp(D)));
set(gca,'XTickLabel',C)



% y axis
ymin=0.05;
ymax=0.99;
yy=(ymin:0.05:ymax); % all data expected to be in this range
set(gca,'YLim',[log(-log(1-ymin)) log(-log(1-ymax))]);% this changes the axis
limits
Dy=log(-log(1-yy));
Dy(19)=log(-log(1-0.96));
Dy=sort(Dy);
set(gca,'YTick',Dy); % defines which ticks are shown but does not change the
axis
Cy={num2str(1-1/exp(exp(Dy(1))));...
    num2str(1-1/exp(exp(Dy(2))));...
    num2str(1-1/exp(exp(Dy(3))));...
    ' ';...
    num2str(1-1/exp(exp(Dy(5))));...
    ' ';...
    ' ';...
    ' ';...
    ' ';...
    num2str(1-1/exp(exp(Dy(10))));...
    ' ';...
    ' ';...
    ' ';...
    ' ';...
    num2str(1-1/exp(exp(Dy(15))));...
    ' ';...
    ' ';...
    num2str(1-1/exp(exp(Dy(18))));...
    num2str(1-1/exp(exp(log(-log(1-0.96)))));...
     };

set(gca,'YTickLabel',Cy)
```